RESEARCH ARTICLE SUMMARY

CANCER GENOMICS

Mechanisms generating cancer genome complexity from a single cell division error

Neil T. Umbreit*†, Cheng-Zhong Zhang*†, Luke D. Lynch‡, Logan J. Blaine‡, Anna M. Cheng, Richard Tourdot, Lili Sun, Hannah F. Almubarak, Kim Judge, Thomas J. Mitchell, Alexander Spektor, David Pellman†

INTRODUCTION: The chromosome breakage-fusion-bridge (BFB) cycle is a catastrophic mutational process, common during tumorigenesis, that results in gene amplification and drives rapid genome evolution. Major mechanisms underlying the BFB cycle are not understood, including its key feature of how chromosome bridges are broken. Furthermore, the simple pattern of DNA sequence rearrangement predicted by the canonical BFB model is not commonly observed in cancer genomes. Instead, the DNA sequence signature of BFB cycles is often accompanied by other genomic rearrangements, including chromothripsis, another catastrophic mutational pattern.

RATIONALE: We recreated essential steps of the BFB cycle in a defined system, enabling mechanistic studies and determination of the immediate and long-term genomic consequences of bridge formation. To identify the immediate outcomes of bridge breakage, we used live-cell imaging coupled with single-cell whole-genome sequencing (Look-Seq). Complex mutational mechanisms, some of which occurred over two generations, could be deconvolved by the comparison of haplotype copy number and structural variants in daughter or granddaughter cells. We then determined the long-term consequences of bridge breakage with genomic analysis of populations derived from single cells after breakage of a bridge formed from an experimentally induced dicentric fusion of chromosome 4.

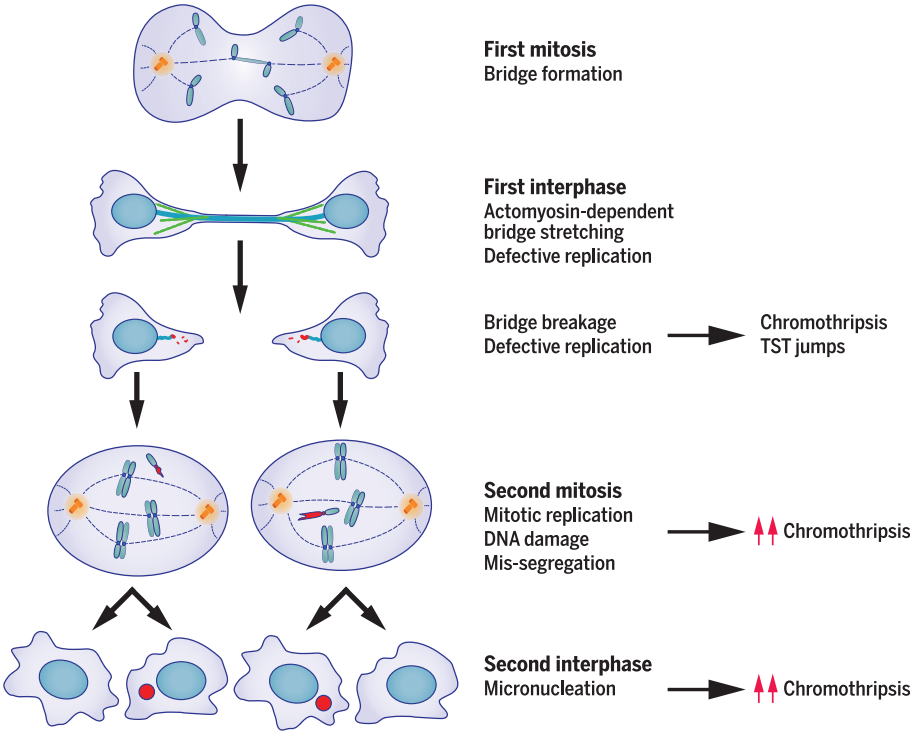

A storm of mutagenesis generates cancer genome complexity from a single cell division error. The interphase actomyosin cytoskeleton (green fibers) stretches and breaks chromosome bridges, promoting local chromosome fragmentation (damaged DNA indicated in red). Defective DNA replication, first during interphase and later in the subsequent mitosis, generates additional DNA damage and chromothripsis, in some instances leaving behind a specific mutational signature (TST jumps). Bridge chromosomes frequently missegregate and form micronuclei, promoting additional chromothripsis.

RESULTS: We showed that chromosome bridge breakage requires actomyosin-dependent mechanical force. Bridge formation and breakage is then coupled to a cascade of additional mutational events. For the initial step, we determined that direct mechanical bridge breakage can generate simple breaks and local DNA fragmentation, providing one explanation for a rearrangement pattern frequently observed in cancer genomes termed "local jumps." Concomitantly, there is defective DNA replication of bridge DNA, which our data suggest can generate complex rearrangements. Some of these rearrangements exhibit a distinct sequence signature of tandem arrays of many short (~200 base pairs) insertions that we term "Tandem Short Template (TST) jumps." We validated the presence of TST jumps in a human cancer by use of single-molecule long-read DNA sequencing. Next, a second wave of DNA damage and increased chromothripsis occurs during the mitosis after bridge formation, when chromosomes from broken bridges undergo an unexpected burst of aberrant DNA replication. Last, these damaged bridge chromosomes missegregate with high frequency and form micronuclei in the following cell cycle, which can generate additional cycles of bridging, micronucleation, and chromothripsis. Genome sequence analysis of clonal populations established that the breakage of chromosome bridges initiates iterative cycles of complex karyotype evolution. We observed an analogous series of events after the formation of micronuclei, suggesting a unifying model for how cancer-associated defects in nuclear architecture ("nuclear atypia") promote genome instability.

ON OUR WEBSITE

Read the full article at http://dx.doi.org/10.1126/science.aba0712

CONCLUSION: We identified a cascade of events that explains how a single cell division error—chromosome bridge formation—can rapidly generate many hallmark features of cancer genomes, including ongoing genome evolution with subclonal heterogeneity. These results motivate a substantial revision of the chromosome BFB model, establishing that episodes of chromothripsis will be inherently interwoven with BFB cycles. These mutational events are common in cancer but likely also occur during development and across organismal evolution. ■

The list of author affiliations is available in the full article online.
*These authors contributed equally to this work.
†Corresponding authors. Email: neilt_umbreit@dfci.harvard.edu (N.T.U.); david_pellman@dfci.harvard.edu (D.P.); cheng-zhong_zhang@dfci.harvard.edu (C.-Z.Z.)
‡These authors contributed equally to this work.
Cite this article as N. T. Umbreit *et al.*, *Science* **368**, eaba0712 (2020). DOI: 10.1126/science.aba0712

RESEARCH ARTICLE

CANCER GENOMICS

Mechanisms generating cancer genome complexity from a single cell division error

Neil T. Umbreit[1,2,3]*†, Cheng-Zhong Zhang[4,5]*†, Luke D. Lynch[2,3]‡, Logan J. Blaine[2,3]‡, Anna M. Cheng[1,2,3], Richard Tourdot[4,5], Lili Sun[6], Hannah F. Almubarak[4,5], Kim Judge[7], Thomas J. Mitchell[7,8], Alexander Spektor[2,3,9], David Pellman[1,2,3]†

The chromosome breakage-fusion-bridge (BFB) cycle is a mutational process that produces gene amplification and genome instability. Signatures of BFB cycles can be observed in cancer genomes alongside chromothripsis, another catastrophic mutational phenomenon. We explain this association by elucidating a mutational cascade that is triggered by a single cell division error—chromosome bridge formation—that rapidly increases genomic complexity. We show that actomyosin forces are required for initial bridge breakage. Chromothripsis accumulates, beginning with aberrant interphase replication of bridge DNA. A subsequent burst of DNA replication in the next mitosis generates extensive DNA damage. During this second cell division, broken bridge chromosomes frequently missegregate and form micronuclei, promoting additional chromothripsis. We propose that iterations of this mutational cascade generate the continuing evolution and subclonal heterogeneity characteristic of many human cancers.

Cancer genomes can contain hundreds of chromosomal rearrangements (*1*). The conventional view is that cancer genomes evolve gradually by accruing small-scale changes successively over many generations. However, the large number of rearrangements in many cancers suggests a nonexclusive, alternative view: Cancer genomes may evolve rapidly through discrete episodes that generate bursts of genomic alterations (*1*–*8*). This model is appealing because a small number of catastrophic mutational events can parsimoniously explain the origin of extreme complexity in many cancer genomes (*4*).

Four classes of catastrophic events may account for a substantial fraction of chromosome alterations in cancer: whole-genome duplication, chromoplexy, chromothripsis, and chromosome breakage-fusion-bridge (BFB) cycles. The first class, whole-genome duplication, can promote tumorigenesis (*3*) and is now appreciated to occur during the development of ~40% of human solid tumors (*9*, *10*). The second class, chromoplexy, is balanced chains of rearrangements between multiple chromosomes (*11*) and is estimated to occur in ~18% of cancers (*1*).

The third class, chromothripsis, is the extensive rearrangement of only one or a few chromosomes, generating a characteristic DNA copy number pattern (*4*, *6*, *12*). Chromothripsis occurs with frequencies of 20 to 65% in certain common tumor types (*1*, *2*, *13*). We previously determined that chromothripsis can originate from micronuclei, which arise from mitotic segregation errors or unrepaired DNA breaks that generate acentric chromosome fragments (*14*–*17*). Because of aberrant nuclear envelope (NE) assembly around these chromosomes, micronuclei undergo defective DNA replication and spontaneous loss of NE integrity, which results in extensive DNA damage from unknown mechanisms (*18*, *19*).

The fourth class of catastrophic event, the chromosome BFB cycle (*20*, *21*), starts with the formation of another abnormal nuclear structure, a chromosome bridge. Bridges arise from end-to-end chromosome fusions after DNA breakage or telomere crisis, incomplete DNA replication, or failed resolution of chromosome catenation (*21*–*25*). Bridge breakage then initiates a process that can generate gene amplification over multiple cell generations. Although BFB cycles are a major source of genome instability, the sequence pattern of consecutive foldback rearrangements expected from the original BFB model is not commonly observed in cancer genomes without other chromosome alterations (*1*, *13*, *26*). Whether subsequent chromosomal rearrangement obscures the simple BFB pattern or whether the BFB process itself is inherently more complex than originally envisioned has been unclear. Recently, examples were identified of cancer genomes in which BFB cycles are intermingled with chromothripsis, raising the possibility that BFB cycles and chromothripsis might be mechanistically related (*26*–*28*).

Determining the generality of the association between chromothripsis and BFB cycles requires knowledge of the detailed mechanisms for each step in the BFB cycle, particularly how chromosome bridges are broken. Proposed mechanisms for chromosome bridge breakage have included breakage by spindle forces during the mitosis in which they are formed or DNA cleavage by the cytokinesis-abscission apparatus (*21*, *29*–*31*). Yet, recent work indicates that breakage of chromosome bridges, at least the "bulky" bridges visible with DNA staining (*32*), is uncommon during mitosis or cytokinesis, and they instead persist for many hours into interphase (*33*, *34*). It was then proposed that interphase bridges are severed by three-prime repair exonuclease 1 (TREX1), which resides in the cytoplasm on the endoplasmic reticulum (*33*). Transient NE disruption was suggested to allow TREX1 to enter the nucleus, where it could simultaneously break the bridge and fragment bridge DNA to generate chromothripsis (*33*). Although the TREX1 model can explain the association between BFB cycles and chromothripsis in cancer genomes (*26*), loss of TREX1 was reported to delay, but not block, bridge breakage (*33*).

We present data that support an alternative model for the genomic consequences of BFB cycles, explaining its association with chromothripsis. Rather than being generated simultaneously by a single mechanism, we demonstrate that chromothripsis accumulates through a cascade of mutational events initiated by the formation of a chromosome bridge. We observed an analogous series of events after the formation of micronuclei, suggesting a unifying model for how cancer-associated defects in nuclear architecture ("nuclear atypia") promote genome instability. Together, these findings reveal how a single cell division error rapidly generates extreme genomic complexity and continually evolving subclonal heterogeneity.

Results

We used four methods to generate chromosome bridges: transient expression of a dominant negative variant of telomeric repeat-binding factor 2 (TRF2-DN) (*22*), partial knockdown of condensin (siSMC2) (*23*), low-dose topoisomerase II inhibition (ICRF-193) (*24*), and CRISPR/Cas9–mediated telomere loss on chromosome 4 (Chr4 bridge) (fig. S1, A to C; a list of bridge-induction methods for each experiment is provided in table S1). Chromosome bridges were visualized in live cells with green fluorescent protein–barrier-to-autointegration factor (GFP-BAF) (*35*), a sensitive reporter for these structures whose signal is not compromised by stretching of the bridge (Fig. 1), unlike fluorescent

[1]Howard Hughes Medical Institute, Chevy Chase, MD, USA. [2]Department of Cell Biology, Harvard Medical School, Boston, MA, USA. [3]Department of Pediatric Oncology, Dana-Farber Cancer Institute, Boston, MA, USA. [4]Department of Biomedical Informatics, Harvard Medical School, Boston, MA, USA. [5]Department of Data Sciences, Dana-Farber Cancer Institute, Boston, MA, USA. [6]Single-Cell Sequencing Program, Dana-Farber Cancer Institute, Boston, MA, USA. [7]Wellcome Sanger Institute, Hinxton, Cambridgeshire CB10 1SA, UK. [8]Cambridge University Hospitals NHS Foundation Trust, Cambridge CB2 0QQ, UK. [9]Department of Radiation Oncology, Dana-Farber Cancer Institute, Boston, MA, USA.
*These authors contributed equally to this work.
†Corresponding authors. Email: neilt_umbreit@dfci.harvard.edu (N.T.U.); david_pellman@dfci.harvard.edu (D.P.); cheng-zhong_zhang@dfci.harvard.edu (C.-Z.Z.)
‡These authors contributed equally to this work.

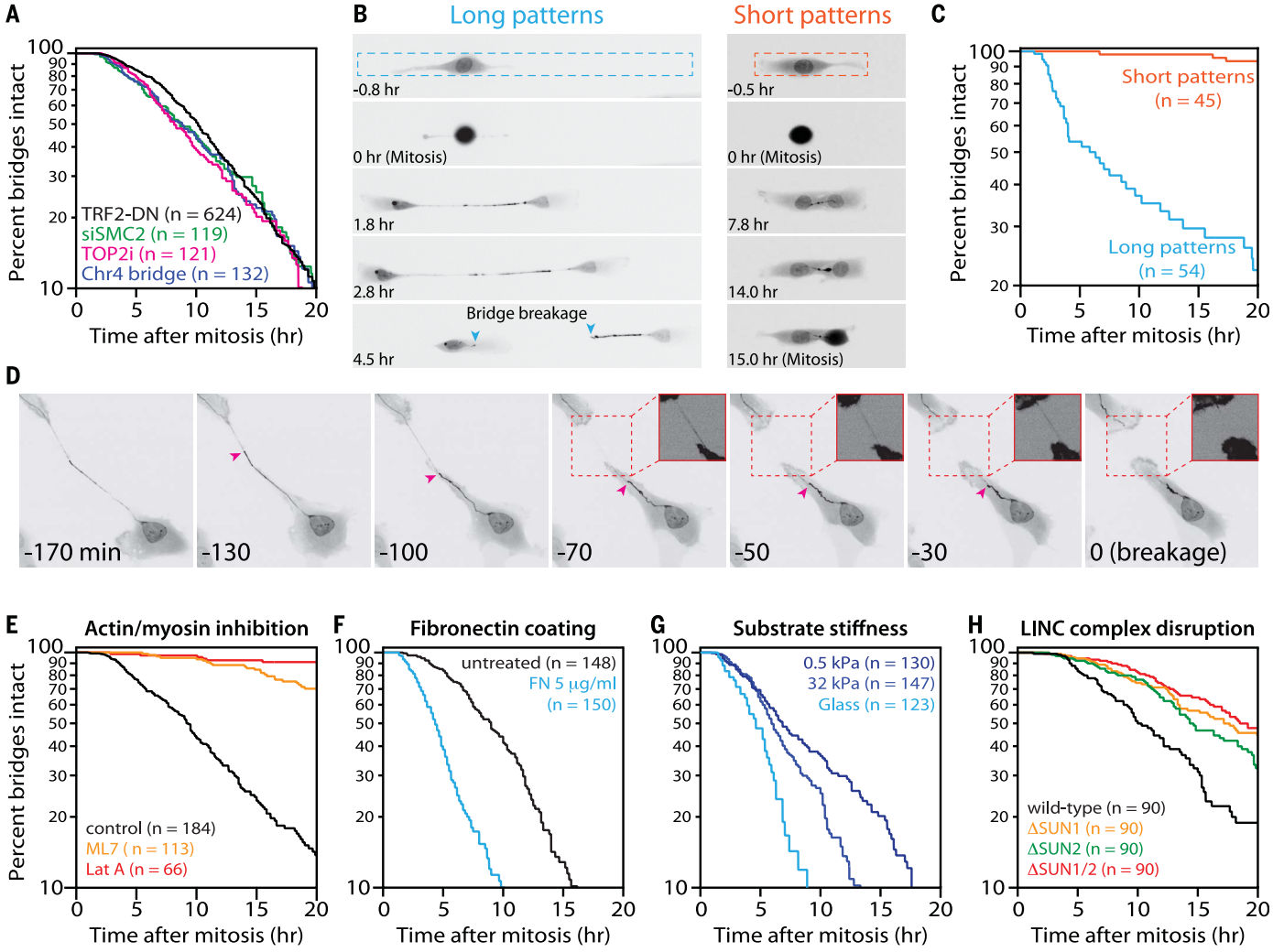

Fig. 1. Chromosome bridge breakage requires actomyosin contractility. (**A**) Indistinguishable chromosome bridge lifetimes observed with different methods for bridge induction. Shown are bridge lifetimes (time from bridge formation until breakage or mitotic entry). Bridges were visualized with GFP-BAF and generated by means of inducible TRF2-DN (n = 624 bridges analyzed), condensin partial knockdown (siSMC2, n = 119), low-dose ICRF-193 (n = 121), or inducible CRISPR/Cas9 cutting of Chr4 subtelomere (n = 132). These mean bridge lifetimes are not significantly different (P = 0.14, one-way analysis of variance). (**B**) Extension of chromosome bridges is required for their breakage. Shown are time-lapse images (GFP-BAF) of cells with bridges on "long" (20 by 300 µm) or "short" (20 by 100 µm) fibronectin (FN) micropatterns. Bridge length does not exceed ~50 µm on short patterns. Dashed lines indicate micropattern borders. Teal arrowheads indicate broken bridge ends. Time stamp is relative to completion of the previous mitosis. (**C**) Quantification from (B): bridge lifetime on short (n = 45) and long (n = 54) micropatterns (P < 0.0001, Mann-Whitney). (**D**) Representative chromosome bridge-breakage event. Before breakage, there is apparent nonuniform stretching of the bridge (GFP-BAF). Magenta arrowheads indicate a transition between "taut" and "slack" regions of the bridge. The taut region progressively stretches, the slack region progressively retracts, and breakage occurs in the taut region. (Insets) High-contrast of the taut region (dashed red boxes) before and after breakage. Time stamp is relative to bridge breakage. (**E**) Actomyosin contractility is required for bridge breakage. Cells were allowed to divide and form bridges before exchange into drug medium (scheme is provided in fig. S5D). Plot shows bridge lifetimes with actin disruption (LatA, n = 66), myosin-II inhibition (ML7, n = 113), and control (DMSO, n = 184). (**F**) Increased cellular contractility decreases bridge lifetime. Bridge lifetimes on untreated glass (n = 148) or FN-coated glass (n = 150). (**G**) Bridge-breakage timing depends on substrate stiffness: glass (>10^6 kPa, n = 123), stiff gel (32 kPa, n = 147), and soft gel (0.5 kPa, n = 130). All substrates were coated with 5 µg/ml FN. (**H**) Partial requirement of LINC complex for bridge breakage: wild-type (n = 90), ΔSUN1 (n = 90), ΔSUN2 (n = 90), and ΔSUN1/ΔSUN2 (n = 90) RPE-1 cells.

histone reporters (*33*). For TRF2-DN, we developed conditions for transient expression and live-cell imaging that avert the previously reported strong inhibition of cell cycle progression (*33*). In our conditions, cells with bridges entered S phase with similar timing after mitotic exit as unperturbed cells lacking bridges (8.3 versus 7.3 hours, respectively) (fig. S1D and accompanying legend). Bridges generated by these different methods had similar median lifetimes ($t_{1/2}$): ~10 hours from the completion of mitosis (Fig. 1A).

Mechanical force triggers chromosome bridge breakage

The TREX1 exonuclease was proposed to cleave chromosome bridges after rupture of the primary nucleus (*33*). In our experimental system, we did not detect a delay in the timing of bridge breakage in cells in which TREX1 was knocked out, even when using the same cell lines and bridge induction method (in total, we used two different bridge-induction methods and tested six independent clones from two knockout strategies) (fig. S2, A to C) (*33*). Additionally, 36% of bridge-breakage events occurred in the absence of detectable rupture of the

primary nucleus (n = 58 bridges analyzed), and bridge lifetime showed no correlation with the duration of NE disruption (fig. S2D). These findings suggested that fundamental aspects of the mechanism for bridge breakage remained to be identified.

A clue to alternative mechanisms unrelated to TREX1 came from the observation that bridges can reach hundreds of micrometers in length before breaking as interphase cells migrate in culture, suggesting that bridge breakage might have a mechanical component. Accordingly, we found that motile cell lines broke bridges during interphase with similar timing, whereas bridges in less motile cell lines almost never extended beyond 100 μm and rarely underwent breakage before the next mitosis (fig. S3).

To determine whether bridge extension is required for breakage, we constrained cell migration and bridge extension using rectangular fibronectin "micropatterns" (*36*). When RPE-1 (retinal pigmented epithelial) cells were plated on long (300 μm) patterns, newly formed chromosome bridges extended to ~160 μm on average and broke during interphase with similar kinetics as in unconstrained cells (Fig. 1, B and C, and movie S1). By contrast, restricting bridge extension with short (100 μm) micropatterns limited bridge extension to <50 μm and almost completely blocked bridge breakage (<10% bridge cleavage before entry into the next mitosis) (Fig. 1, B and C, and movie S2). There was also less spontaneous NE rupture on short patterns, but increasing NE ruptures greater than eightfold with Lamin B1 knockdown failed to accelerate bridge breakage (fig. S4). Therefore, the extension of chromosome bridges, but not NE rupture, is required for their breakage.

Mechanical forces could stretch a bridge across its length or act locally within a section of a bridge. Consistent with the latter model, bridges often formed acute angle bends and/or exhibited nonuniform stretching before breakage, with one segment appearing taut and adjacent segments appearing slack, followed by breakage within the taut segment (23 of 25 cases examined) (Fig. 1D and movie S3). Moreover, live-cell imaging revealed the accumulation of large concentrations of actin filaments immediately adjacent to the taut segments of the bridge just before breakage in all cases examined (n = 30 bridges) (fig. S5A and movie S4) [similar results can be found in (*34*)]. Actin accumulations were transient and dissolved after bridge breakage. Large focal adhesions and active, phosphorylated myosin II were also observed at these sites (fig. S5, B and C), which is consistent with local myosin accumulation and high contractility induced by increased membrane tension (*37*) and indicates strong cell attachments to the extracellular matrix.

To determine whether actomyosin contractility is required for chromosome bridge breakage, chromosome bridges were generated, allowed to extend, and exposed to small-molecule inhibitors of myosin activation (ML7) or actin assembly [Latrunculin A (LatA)]. ML7 addition substantially delayed, and LatA addition abolished, bridge breakage (Fig. 1E, fig. S5D, and movie S5). Although LatA blocks cell motility and thus prevents further bridge extension after drug addition, ML7 treatment did not have a significant effect on bridge extension [bridge length before breakage or entry into the next mitosis, mean ± SEM: ML7, 140 ± 11 μm, dimethyl sulfoxide (DMSO), 150 ± 12 μm; P = 0.56, Mann-Whitney test]. Therefore, the prolonged bridge lifetime in ML7-treated cells cannot be explained by an inability to extend bridges. These findings demonstrate that a functional actomyosin network is essential for bridge breakage. Moreover, when cells were plated on fibronectin, which increases focal adhesions and intracellular actomyosin contractile forces (*38*), bridge breakage was accelerated twofold (P < 0.0001) (Fig. 1F). Because fibronectin also affects cell signaling (*39*), we plated cells on hydrogels of varying stiffness, all coated with the same concentration of fibronectin. Consistent with reduced substrate stiffness causing diminished actomyosin contractility (*40*), bridge lifetime was prolonged on softer substrates (Fig. 1G). Last, knockout of SUN1 and SUN2, the major inner nuclear membrane LINC components that transmit actomyosin forces across the NE (*41*), caused a partial delay in bridge breakage ($t_{1/2}$ = 18 hours) (Fig. 1H and fig. S6). Together, these data establish a critical role for cytoplasmic actomyosin contractile forces in chromosome bridge breakage.

Single-cell sequencing to determine the immediate effect of chromosome bridge breakage

Copy number alterations immediately after bridge breakage

To identify the immediate outcome(s) of bridge breakage without confounding genomic alterations during subsequent cell divisions, we used a combination of live-cell imaging with single-cell whole-genome sequencing (Look-Seq) (*17*). Chromosome bridges were induced, their breakage was monitored, and the two daughter cells were isolated ~8 hours after bridge breakage for sequencing (Fig. 2A). Sequencing was performed to ~25× genome coverage, covering ~90% of the specific sequence of each homologous chromosome with one or more reads (supplementary materials, materials and methods).

The BFB model (*21*) predicts that daughter cells should exhibit reciprocal terminal chromosome segment gain and loss patterns because of breakage of dicentric fusions of sister chromatids or single chromatids from different chromosomes ("chromatid-type fusions") (Fig. 2B). In all 20 daughter cell pairs after bridge breakage, we observed reciprocal exchange affecting a segment (>2.5 Mb) of one or more chromosome arms (fig. S7). Using previously developed haplotype copy number analysis (*17*), we could unambiguously identify the homologous chromosome(s) that underwent breakage. Unexpectedly, in four daughter cell pairs, we observed the reciprocal gain and loss of internal chromosome segments. This pattern can be explained by bridge breakage when a pair of dicentric fusions composed of the replicated chromatids from two different chromosomes is formed ("chromosome-type fusions") (Fig. 2C) (*42*). In this circumstance, internal chromosome segment exchange results if kinetochore-microtubule attachments occur in a way that generates an antiparallel orientation of the paired dicentrics. Without information from both daughter cells, the internal segment gain in one daughter could be misinterpreted as replication-based sequence duplication rather than chromosome breakage (supplementary materials, supplementary text). Although bridge breakage sometimes affected only one chromosome, in nine cases, two or more different chromosomes were involved, as expected from the methods used to induce bridges (*43*); the exception was the CRISPR-based method, which exclusively produced chromosome 4 bridges as expected (fig. S7).

Closer inspection of the bridge breakpoints revealed a spectrum of copy number alterations near the break: Some bridges underwent simple breakage, and others experienced fragmentation localized to the region of the main copy number transition (Fig. 3). In cases in which bridge breakage occurred with local fragmentation, fragments as small as ~100 kb could be detected with confidence if these fragments were retained within a larger region of complete haplotype loss. Rearrangements involving fragment ends often provided additional support for these copy number alterations (supplementary materials, materials and methods).

To determine whether simple breaks and local fragmentation can be directly generated by mechanical force, we used a glass capillary to mechanically break chromosome bridges (movie S6). This yielded both simple breaks and local fragmentation (Fig. 4A and fig. S8A). Moreover, we observed similar local fragmentation patterns for spontaneous bridge breakage in TREX1-null cells, reinforcing the conclusion that TREX1 is not required to break or fragment chromosome bridges (Fig. 4B and fig. S8B).

These findings demonstrate that the immediate genomic consequences of bridge breakage are relatively simple patterns of copy number alterations localized near the site(s) of breakage

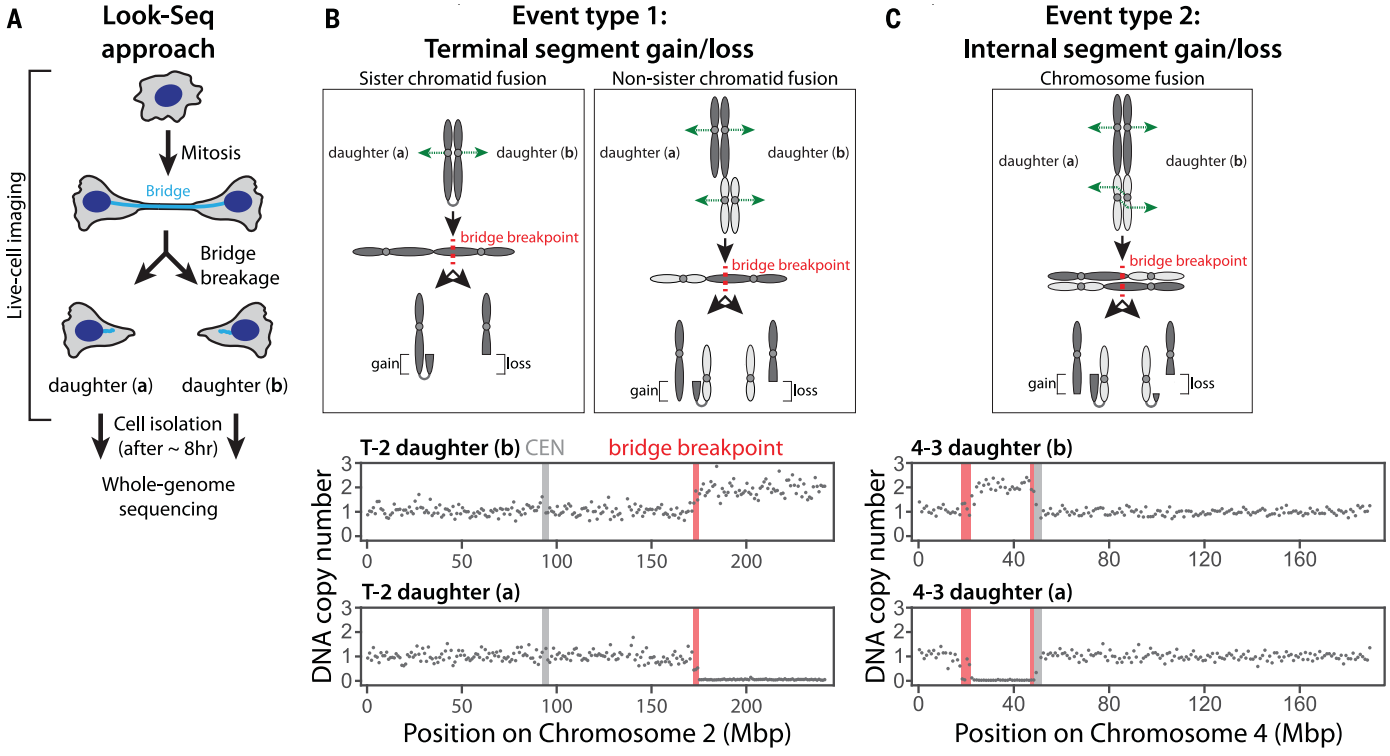

Fig. 2. Immediate effect of chromosome bridge breakage on DNA copy number. (**A**) Illustration of Look-Seq experiments. (**B**) Type 1 events are daughter cells with reciprocal gain and loss of a terminal chromosome segment. (Top) Sister (left) and Non-sister (right) chromatid fusions. In mitosis, the resulting dicentrics are segregated (green dashed arrows), forming a bridge. Bridge breakage (dashed red line) produces copy-number alterations as shown. (Bottom) Representative copy-number plot (gray dots, 1-Mb bins for the affected Chr2 haplotype). The red bar indicates inferred bridge breakpoint. The light gray bar indicates centromere. (**C**) Type 2 events are reciprocal gain and loss of an internal chromosome segment between the daughter cells. (Top) A chromosome fusion (*42*). If the kinetochores of each dicentric attach to microtubules from opposite poles as shown (dashed green arrows), the dicentric chromatids invert relative to each other. Cleavage of the antiparallel chromatid pair yields reciprocal copy number alterations of an internal chromosome segment. (Bottom) DNA copy-number plot as in (B).

on bridge chromosomes. This localized pattern contrasts with what is observed in bulk populations of cells isolated many generations after telomere crisis; these populations often contained complex copy number alterations and rearrangements that encompassed most of a chromosome arm and/or spanned the centromere (*33*). We observed similar complex patterns in long-term population evolution experiments and will present evidence that defines a cascade of events downstream of initial bridge breakage that can explain them (fig. S23).

Chromosome rearrangements associated with bridge breakage

We next analyzed chromosome rearrangements associated with the above-described DNA copy number alterations. Many cell pairs exhibiting local fragmentation contained rearrangements expected from ligation of the fragments (Fig. 3B). In some cases, local fragmentation affected two or more bridge chromosomes, leading to both inter- and intrachromosomal rearrangements (Fig. 3C, bottom cell). This pattern of rearrangements resembles the "local n-jump" or "local-distant" rearrangement clusters identified from a recent analysis of structural variation in cancer genomes (*44*). Therefore, at least some of these patterns (hereafter, "local jumps") likely occur through chromosome fragmentation and DNA ligation, in common with rearrangements meeting conventional criteria for chromothripsis. Thus, consistent with our previous proposal, the mechanisms that generate chromothripsis can also produce less extreme outcomes, suggesting that the frequency of chromothripsis-like phenomena in cancer genomes may be underestimated (*17*).

Tandem Short Template (TST) jumps

Four daughter cell pairs showed a distinct and particularly striking pattern of complex rearrangement (n = 4 of 20 cell pairs) (Fig. 5A). Additionally, two of these cases also evidenced kataegis, a phenomenon in which local clusters of point mutations are generated by APOBEC (apolipoprotein B mRNA editing enzyme, catalytic polypeptide-like) family cytosine deaminases on single-stranded DNA (ssDNA) (fig. S9) (*33*, *45*, *46*). The rearrangement junctions from these four samples had features that are inconsistent with an origin from simple fragmentation followed by ligation in random order and orientation. Instead, this pattern suggests an origin from errors during DNA replication. First, rather than being randomly distributed, breakpoints were tightly clustered into local 1- to 10-kb hotspots (fig. S10A). Second, tracking the connections between rearrangements revealed chains of tandemly arrayed short insertions [median insertion size, 183 base pairs (bp)] (fig. S10B), which we refer to as "Tandem Short Template" (TST) jumps (Fig. 5). The TST insertions typically originated from break ends generated by local fragmentation within the bridge but were occasionally derived from intact chromosomes not obviously in the bridge.

TST jumps might be generated from template-switching errors in DNA replication, as in the microhomology-mediated break-induced replication (MMBIR) model (*12*, *47*). Accordingly, we analyzed microhomology at the junctions between TST insertions. Although a minority of junctions showed blunt end–joining, junctions with obvious microhomology were also infrequent. For example, of the 13 junctions in one TST chain shown in Fig. 5A, five were blunt-end joins (microhomology or

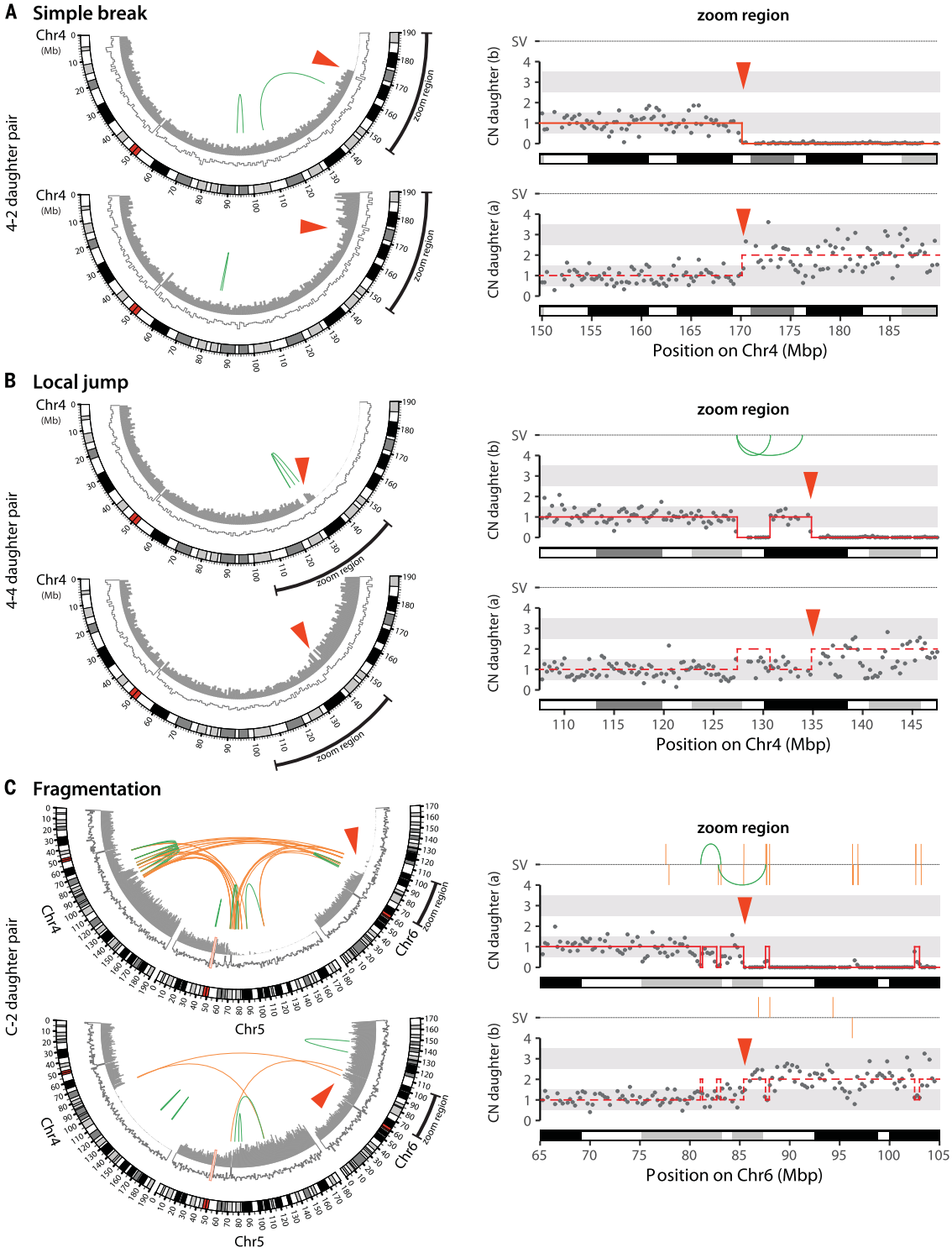

Fig. 3. Localized DNA breakage and rearrangement with bridge breakage. (**A**) Simple bridge breakage. (Left) Circos plots showing the bridge chromosome (Chr4) (*80*). Outer arc indicates the chromosome cytoband. Inner arcs indicate the DNA copy number for the bridge haplotype (solid gray bars) and the nonbridge haplotype (white bars, gray outline). Green lines indicate intrachromosomal structural variants (SVs). Red arrowheads indicate bridge breakpoint. (Right) Zoom-region plot shows copy number (gray dots; 250-kb bins) near the bridge breakpoint. Copy-number segments [solid red lines, (A) to (C)] were determined by using single-nucleotide polymorphism–level coverage in the top daughter (supplementary materials, materials and methods); the bottom daughter is inferred to contain reciprocal copy-number segments [dashed red lines, (A) to (C)]. SVs, as in Circos plots, are shown above. (**B**) Bridge breakage can produce the local jump pattern. As in (A), Circos plots (left) and zoom-region plot (right) for the bridge chromosome (Chr4). (**C**) Local fragmentation and complex rearrangement with bridge breakage. As in (A), CIRCOS plots (left) and zoom-region plot (right) for a bridge containing three different chromosomes (Chr4, Chr5, and Chr6) showing local fragmentation. The pattern of rearrangements in daughter (b) indicates end-joining of these fragments, producing intra- and interchromosomal rearrangements (green and orange lines, respectively). Daughter (a) additionally evidences the TST jump rearrangement pattern (Fig. 5).

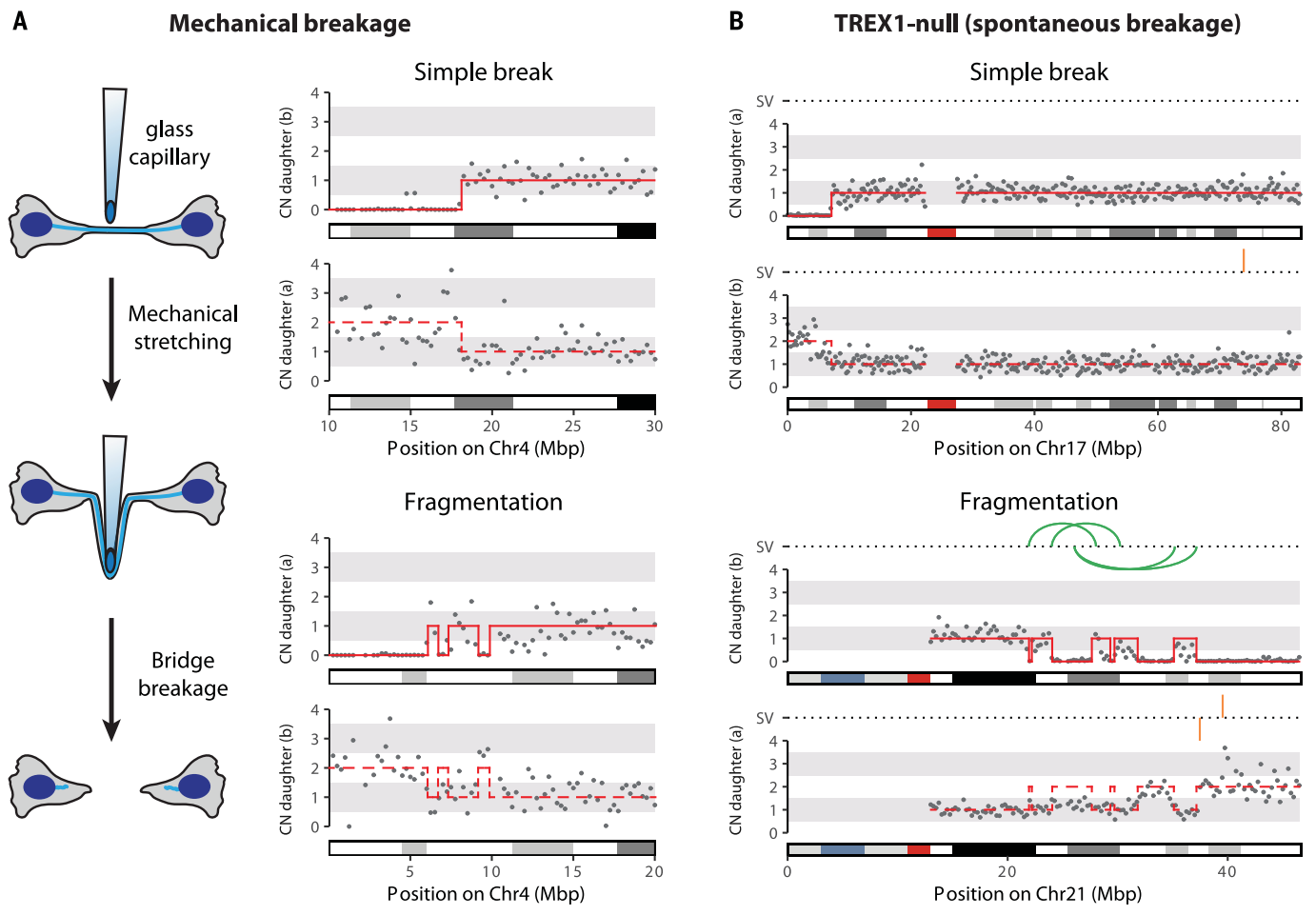

Fig. 4. Local fragmentation accompanies mechanical bridge breakage and does not require TREX1. (**A**) Mechanical bridge breakage produces simple breaks and local fragmentation. (Left) Schematic of the experiment. Cells were collected immediately after mechanical bridge breakage to determine its direct consequences (not allowing time to generate chromosomal rearrangements). (Right) Copy-number plots, as in Fig. 3, show examples of simple bridge breakage (top) and local fragmentation (bottom). (**B**) Copy-number and SV plots, as in Fig. 3: simple bridge breakage (top) and local fragmentation (bottom) after spontaneous bridge breakage in TREX1-null cells.

insertion of ≤1 bp), and two showed microhomology (≥2 bp). The remaining six junctions contained 2 to 20 bp of sequence with ambiguous origin. It is possible that these sequences have junctional microhomology that cannot be detected because the homologous sequences are derived from repeats and/or contain partial mismatches, making them difficult to map (*48*).

In light of these findings, we characterized the efficiency of DNA replication in chromosome bridges by pulse-labeling with the nucleoside analog, 5-ethynyl-2′-deoxyuridine (EdU). In contrast with primary nuclei, in S phase cells, EdU intensity dropped off in the bridge, where it emerged from the main nucleus and was mostly absent from the remainder of the bridge (fig. S11A). Likewise, broken-bridge stubs also displayed defective DNA replication (fig. S11A). Control experiments demonstrated that the absence of EdU signal was not simply a consequence of limited detection sensitivity for the small amount of DNA in bridges (fig. S11B). Moreover, defective replication of bridge DNA could also be inferred from our single cell sequencing data (fig. S11C). Thus, chromosome bridges exhibit severe DNA replication defects similar to those previously identified in micronuclei (*14*, *16*, *19*).

We observed the TST jump signature in two additional contexts, using different sequencing methods. First, we identified the TST jump signature through bulk sequencing of a population of cells derived from a single cell with a broken bridge. We induced the formation of CRISPR-generated Chr4 bridges, isolated individual cells after bridge breakage, and then grew each cell into a large population (>10^6 cells). The TST jump signature, with 150 bp median insertion size, was identified in one of 12 populations (Fig. 5B and fig. S10B), and another sample (sequenced to lower depth) displayed the characteristic breakpoint clustering. Second, we identified the TST jump signature in a tumor genome by means of single-molecule long-read sequencing of a primary tumor sample obtained from a patient with renal cell carcinoma. In this patient sample, the TST jumps are associated with a chromothripsis event between Chr3p and Chr5q (Fig. 5C). This unbalanced translocation is the single most common mechanism underlying Chr3p loss, the canonical driver event in this cancer type (*49*). Again, the size of the insertions (median 199 bp) in the tumor was similar to what we observed with single-cell sequencing of broken bridges (fig. S10B). The TST jump signature therefore reflects a specific mutational process that can be stably inherited over many generations and is present in human primary tumors.

Therefore, sequencing cells after the breakage of chromosome bridges demonstrates that most rearrangements result from ligation after localized fragmentation, but that highly complex rearrangements can occur in a minority

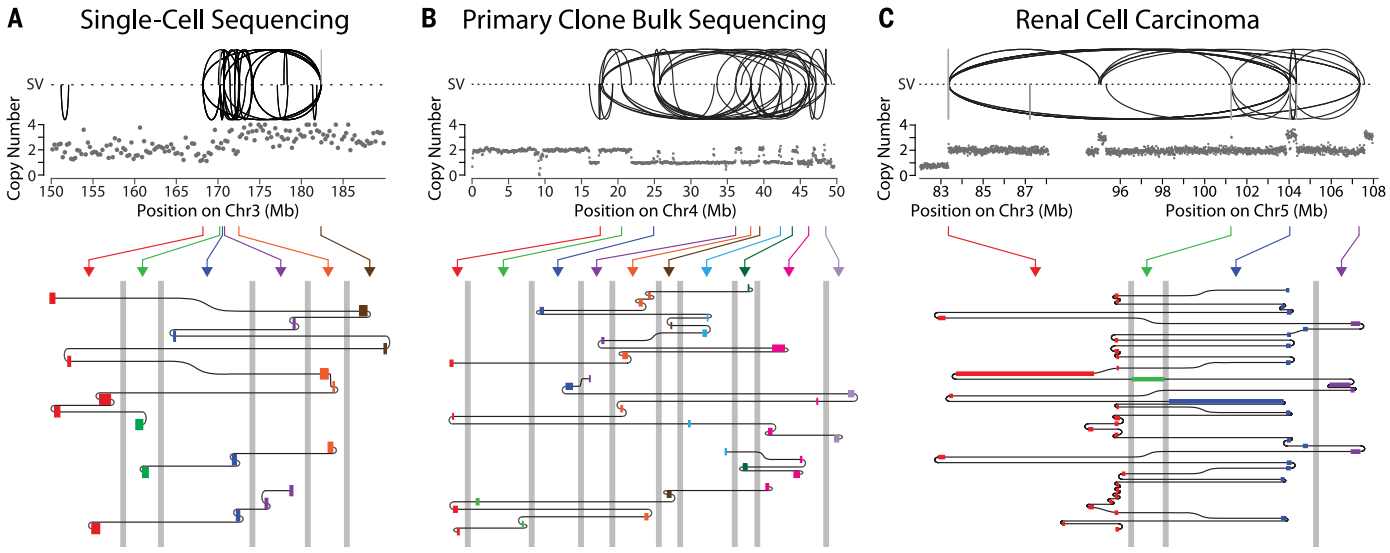

Fig. 5. The TST jump rearrangement signature. (**A**) Features of the TST jump signature. (Top) Plots show copy number (gray dots, 250-kb bins) and SVs (black, intrachromosomal; gray, interchromosomal) for a region near the bridge breakpoint on Chr3. (Bottom) Schematic shows three chains of templated insertions (rectangles), colored according to their origin from six breakpoint hotspots (arrows from top). Templated insertions are connected as shown by black lines, in a zoom-region view for each breakpoint hotspot (≤10-kb window in each region). Gray vertical lines are axis breaks indicating distances of >10 kb between the hotspots. (**B**) The TST jump signature in bulk sequencing data from a primary clone after bridge breakage. (Top) Copy number (250-kb bins) and SVs for the bridge chromosome (Chr4). (Bottom) Four chains of templated insertions originating from 10 breakpoint hotspots. (**C**) TST jump signature in long-read sequencing from a renal cell carcinoma sample. (Top) Copy number (10-kb bins) and SVs for the region of unbalanced translocation between Chr3 and Chr5. (Bottom) One chain of templated insertions originating from four breakpoint hotspots (3- to 10-kb windows).

of cases. The sequence features of these rearrangements (TST jumps) suggest an origin from template-switching errors in DNA replication (*12*, *48*, *50*, *51*).

Mechanisms generating DNA damage downstream of chromosome bridge breakage

Damage from aberrant mitotic DNA replication

Although there is only a low frequency of complex rearrangement associated with the initial formation and breakage of chromosome bridges in the first generation, complex rearrangements appeared to arise frequently in the second generation (granddaughter cells, the progeny of daughter cells with broken chromosome bridges). In all three of the second-generation lineages examined by means of single-cell sequencing, we detected chromothripsis-like rearrangements localized near the bridge breakpoints (fig. S12). This suggested that the broken stubs of chromosome bridges might acquire additional damage during passage through mitosis.

We assayed DNA damage in mitosis using a protocol of live-cell imaging followed by fixation and staining for γ–H2A histone family member X (γ-H2AX) in these same cells. Relative to primary nuclei, most broken bridges exhibited little or no damage during interphase, even when cells were held in extended G_2-arrest with cyclin-dependent kinase 1 (Cdk1) inhibition. However, if cells with broken-bridge stubs were released from G_2-arrest into mitosis, γ-H2AX labeling intensity increased approximately fivefold (Fig. 6, A and B). Heavy mitotic γ-H2AX labeling was consistently associated with extensive replication protein A (RPA) accumulation, indicating the generation of ssDNA (Fig. 6, A and B, and fig. S13A). Surprisingly, pulse-labeling with EdU revealed that RPA and γ-H2AX accumulation coincided with extensive DNA synthesis that occurred specifically on the bridge DNA during mitosis (Fig. 6C). Similar findings were obtained in BJ cells (fig. S13B). Live-cell imaging of GFP-RPA2 established that the mitotic replication was restricted to the stub of the broken chromosome bridge (fig. S13A and movie S7). Therefore, the stubs of broken chromosome bridges undergo a second wave of DNA damage during a burst of aberrant, mitosis-specific DNA replication.

Chromosome bridges generate micronuclei

If chromosome bridge formation generated micronuclei, the frequency of chromothripsis and the size of the rearrangement footprint would be further increased (*14*, *17*). This could contribute to the extensive pattern of rearrangements previously reported by means of bulk sequencing of cell clones derived after telomere crisis (*33*).

Although it was recently reported that micronuclei do not form immediately after chromosome bridge breakage (*33*), whether the resulting broken chromosomes segregate normally in subsequent cell divisions has not been examined. We therefore used live-cell imaging to track bridge chromosomes over two generations (Fig. 6D). Our imaging confirmed that micronucleation is not an immediate consequence of chromosome bridge breakage in the interphase during which the bridge forms and breaks. However, a different result was obtained when cells with broken bridges went through the next mitosis: 52% of divisions resulted in granddaughter cells with micronuclei (n = 82 daughter cell divisions examined) (Fig. 6D and fig. S14A). When the bridge did not break during the first cell cycle, the frequency of micronucleation was higher still (65%, n = 20 divisions) (fig. S14B). By comparison, cells without a bridge divided normally and did not produce micronuclei (n = 82 divisions), even though they were present in the same imaging dish and were treated identically.

To determine whether the above-described micronuclei contain chromosomes from bridges, we induced CRISPR-generated Chr4 bridges and used fluorescence in situ hybridization (FISH) to detect DNA from Chr4. After induction, almost all bridges contained Chr4 sequence, and in the second cell cycle, most micronuclei contained DNA from Chr4 (80%, n = 105 micronucleated cells) (fig. S14C). Surprisingly, and in contrast to an early model based on a different cell line (*52*), most of these micronuclei also contained Chr4 centromere DNA (62%, n = 84 micronuclei containing Chr4 DNA), suggesting that bridge formation and/or

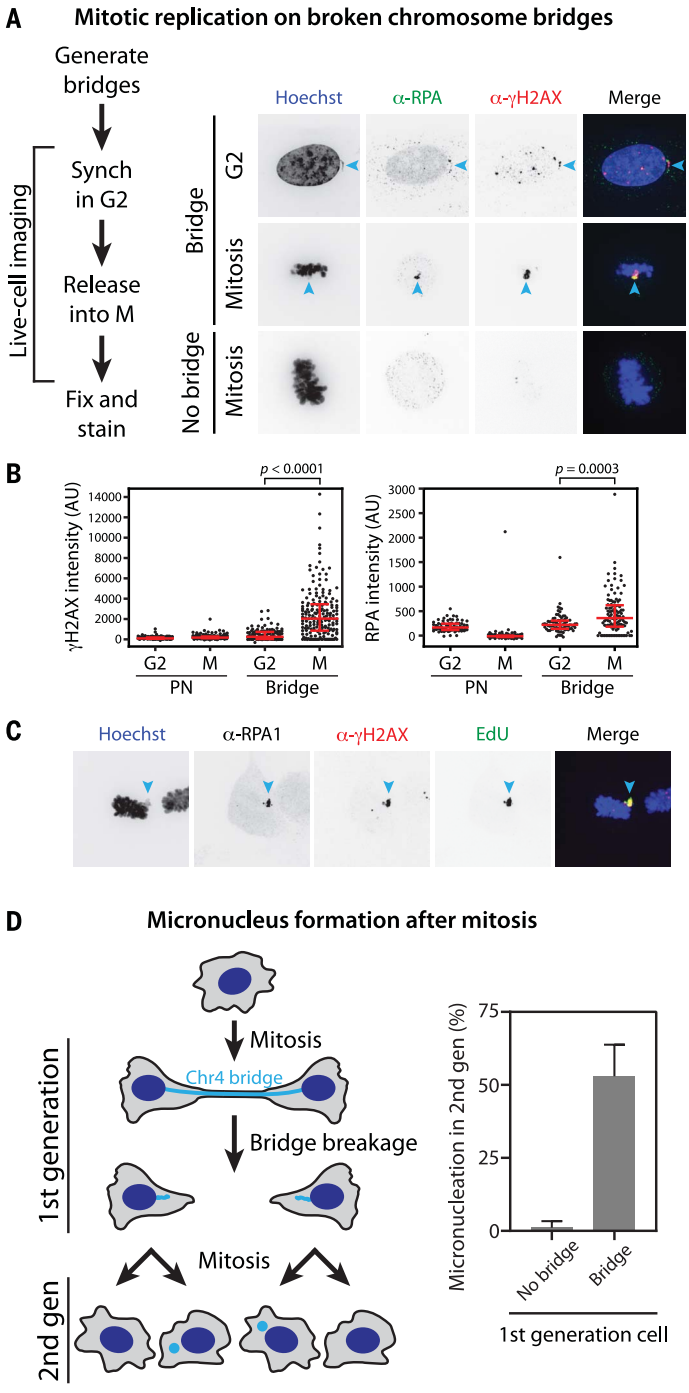

Fig. 6. Broken bridge chromosomes undergo mitotic DNA damage and frequent missegregation to form micronuclei. (**A**) Mitosis-specific damage of bridge DNA detected with correlative live-cell/same-cell fixed imaging. (Left) Schematic of the experiment. (Right) Example images of cells with broken bridges in G_2 or in mitosis, compared with a control mitotic cell (no bridge in the prior interphase). Cyan arrowheads indicate bridge chromosome. (**B**) Quantification from (A); *P* values from Mann-Whitney test. (**C**) DNA damage (γ-H2AX) coincides with RPA accumulation and active DNA replication (EdU). Cyan arrowheads indicate bridge chromosome. (**D**) Frequent micronucleation in the second generation after bridge formation. (Left) Schematic of the live-cell imaging experiment. A cell divides, forming a CRISPR-induced Chr4 bridge (first generation). After bridge breakage, daughter cells divide, forming "granddaughter" cells (second generation). (Right) Frequency of micronucleation in second-generation cells was measured for control cells that did not have a bridge in the first generation (No bridge) as compared with cells that did (Bridge).

breakage disrupts centromere function. Thus, micronucleation is a major downstream consequence of chromosome bridge formation, regardless of whether the bridge breaks.

Common mechanisms for DNA damage in micronuclei and chromosome bridges

Because micronuclei and chromosome bridges share a common NE defect (*19*), we hypothesized that these structures, although differing morphologically, might nevertheless have a similarly defective nucleoplasm leading to defects in DNA replication—both during interphase and then later in mitosis. As a first step, we addressed whether micronuclei acquire replication-dependent DNA damage during interphase. Because NE disruption itself causes DNA damage (*18*), we characterized micronuclei with intact NEs, identified by the accumulation of nuclear-targeted red fluorescent protein (RFP-NLS) (*18*).

Micronuclei were generated by means of a nocodazole washout procedure (*17*), and we used EdU-labeling to assess the extent of DNA replication in micronuclei. Relative to the primary nucleus, many intact micronuclei in G_2 cells showed detectable but strongly reduced DNA replication, as expected (median EdU ratio = 27%). DNA damage was observed in a subset of intact micronuclei (23%), almost exclusively in micronuclei with the strongest replication defect (fig. S15, A and B), suggesting that DNA damage is coupled to defective replication. Furthermore, DNA damage was nearly eliminated by blocking the initiation of DNA replication with small-molecule inhibitors of either cyclin-dependent kinase (CDK) or Dbf4-dependent kinase (fig. S15, A and B). Although γ-H2AX intensity measurements were reliable for assessing DNA damage in micronuclei, similar measurements are not feasible for chromosome bridges because of the tension-induced depletion of nucleosomes from stretched bridges (*33*). Single-cell sequencing showed extensive chromothripsis-like rearrangements in 1 of 10 G_2 cells with intact micronuclei (fig. S15C). Thus, like chromosome bridges, intact micronuclei undergo defective DNA replication in interphase during the first cell cycle after their formation, which appears to generate a low frequency of DNA damage and chromothripsis.

We next determined whether micronuclear chromosomes, like broken chromosome bridges, undergo mitotic replication and secondary DNA damage. Although most intact micronuclei in G_2 cells lacked DNA damage, after entering mitosis, there was a ~10-fold increase in damage levels on micronuclear chromosomes, accompanied by mitotic DNA synthesis and the extensive accumulation of ssDNA (fig. S16 and movie S8).

Single-cell sequencing demonstrated that transit through mitosis promotes chromothripsis of micronuclear chromosomes. By use

of live-cell imaging, we identified cells with intact micronuclei that subsequently went through mitosis, generating daughter cells. In contrast with parental G_2 cells, where chromothripsis was rare (1 of 10 cells) (fig. S15C), chromothripsis was common in these daughter cells that had passed through mitosis (8 of 9 cell pairs, $P = 0.001$, Fisher's exact test) (fig. S16D). Thus, incompletely replicated chromosomes from either micronuclei or bridges undergo aberrant replication upon entry into mitosis, correlated with a high frequency of chromothripsis in the next generation.

Therefore, at a low frequency, DNA from chromosome bridges or micronuclei undergoes fragmentation and rearrangement during defective DNA replication in interphase. Subsequently, a second wave of abnormal replication and heavy DNA damage occurs when cells enter mitosis. After mitosis, DNA damage and chromothripsis can be further amplified on bridge chromosomes by their frequent missegregation into micronuclei.

Complex genome evolution from the formation of a chromosome bridge

The above-described findings predict that the formation of a chromosome bridge should initiate ongoing genome instability (*53*) in which episodes of chromothripsis would necessarily occur at multiple steps of the BFB cycles (*4*, *27*).

To test this model, we tracked the evolution of CRISPR-generated Chr4 bridges during long-term population growth. The parental line without CRISPR induction did not show alterations to Chr4 and maintained a stable karyotype (table S2). By contrast, each of 12 clones isolated downstream of initial bridge formation and breakage (hereafter, "primary clones") contained an altered Chr4 according to cytogenetic analysis (table S2). Additionally, bulk genome sequencing revealed copy number alterations that affected one or both homologs of Chr4 in each primary clone (Fig. 7A and fig. S17).

In addition to the Chr4 aberrations, the primary clones had a total of 26 karyotype abnormalities affecting other chromosomes (table S2). Nearly all non-Chr4 aberrations involved acrocentric chromosomes (85% of cases) (table S2), usually fused at their p-arms to an abnormal Chr4 (fig. S18). This is unlikely to have resulted from off-target CRISPR cutting because acrocentric fusions are also common in RPE-1 cells after TRF2-DN–mediated bridge induction (*54*). Acrocentric chromosomes may be frequently fused to other broken chromosomes because their p-arm rDNA repeats are fragile (*55*) or because fusion to an acrocentric chromosome is more likely to generate a single centromere. The non-Chr4 aberrations were typically subclonal within each primary clone (fig. S18 and table S2), suggesting downstream evolution after breakage of the Chr4 bridge.

Ongoing genome instability within most of the primary clones was further supported by (i) high frequencies of micronuclei and chromosome bridges and (ii) noninteger copy-number states in the bulk sequencing data, indicating subclonal copy-number heterogeneity (Fig. 7A and fig. S19). Genetic heterogeneity between cells in the primary clones was directly verified by performing single-cell copy-number profiling (500 to 800 cells from each clone) (Fig. 7B and fig. S20). Extensive copy-number variation was observed, mostly confined to Chr4 but also on acrocentric Chrs 13, 14, 15, and 22 (Data materials and availability, Dryad; Fig. 7B; and fig. S20).

To better understand the evolution of copy number variation, we performed bulk whole-genome sequencing on subclones derived from single cells isolated from the primary clones (Fig. 7, C and D). Analysis of these subclones provided clear evidence that complex chromosomal rearrangements occur downstream of bridge breakage.

First, in one set of subclones (derived from primary clone 2a) with copy number profiles exhibiting a single, shared ancestral breakpoint, we also identified additional breakpoints that occurred only within specific lineages (Fig. 7C). These breakpoints private to each lineage can only have been acquired after the shared ancestral break.

Second, in a different set of subclones (from primary clone 1a), we observed kataegis in 22 of 23 subclones; however, only a minority of these kataegis events were shared among all the subclones (fig. S21). Most kataegis events were identified in only a subset of subclones or were private to just one subclone (fig. S21), suggesting that they arose late during population expansion.

Third, among this same set of subclones, we observed variation in both the location and the magnitude of focal amplifications on Chr4 homolog A (fig. S22). BFB cycles are not conventionally considered to be mechanisms for internal-chromosome focal amplification; however, we suggest that this could occur if bridge fragments are ligated to form extrachromosomal circles (*17*).

Fourth, among nine subclones that shared a common copy-number profile of homolog A (fig. S22, top profile), there was variable loss of homolog B from the p-arm terminus, a pattern that is suggestive of progressive shortening (Fig. 7D). These findings suggest that subclonal loss of homolog B occurred late during growth of the primary clone, postdating the alterations of homolog A. In this example, the apparent progressive shortening of homolog B likely reflects ongoing BFB cycles. The absence of cells with gain of this region, as expected from the original BFB model, could result from compromised fitness of cells with Chr4 terminal-segment gene amplification and/or a bias toward segmental loss owing to underreplication of bridge DNA (fig. S11). This progressive terminal segment loss generates a characteristic gradual, sloping copy-number transition in the bulk sequencing data (Fig. 7D). This pattern is apparent in several of our primary clones (fig. S19). We suggest that this pattern may provide a useful bulk DNA sequence–based biomarker of ongoing genome instability.

Discussion

Our results identify a cascade of events that generate increasing amounts of chromothripsis after the formation of a chromosome bridge, creating many hallmark features of cancer genomes from a single cell division error. We demonstrate that episodes of chromothripsis will be inherently interwoven with multiple steps of the BFB cycle. This motivates a revision of the chromosome BFB model (*20*, *21*, *56*) that explains the inferred association between these processes in cancer genomes.

We propose the following model (fig. S23). Like micronuclei, NE assembly around chromosome bridges is aberrant, leading to depletion of nuclear pores (*4*, *19*, *52*), which combined with bridge geometry (*57*) leads to a defective nucleoplasm. This results in poor DNA replication in the bridge, producing stalled replication forks and replication origins that have not fired. The bridge is then broken by a mechanism that requires stretching force from the actin cytoskeleton. Bridge breakage produces simple breaks and local fragmentation, generating free DNA ends that can engage in end-joining and/or in error-prone replicative repair, potentially MMBIR (*10*, *47*). In some cells, this produces the rearrangement signature that we term TST jumps. These events lead to a low frequency of chromothripsis during the interphase, in which the bridge forms and breaks. Subsequently, after cells enter mitosis, the stubs of broken chromosome bridges undergo a burst of aberrant mitotic DNA replication, similar to what occurs for micronuclear chromosomes. This leads to significantly more DNA damage and increases the frequency of chromothripsis. Last, bridge formation compromises centromere function, which increases the rate of micronucleation during the next cell division after bridge formation. These micronuclei will generate further cycles of chromothripsis, as previously described (*14*, *15*, *17*). Combined, these mutational events rapidly generate hallmark features of cancer genome complexity, producing continuing cycles of genome evolution and ongoing subclonal heterogeneity from a single cell division error.

Mutagenesis and DNA fragmentation from actomyosin-based force

It was previously proposed that bridge breakage might occur because of mechanical forces

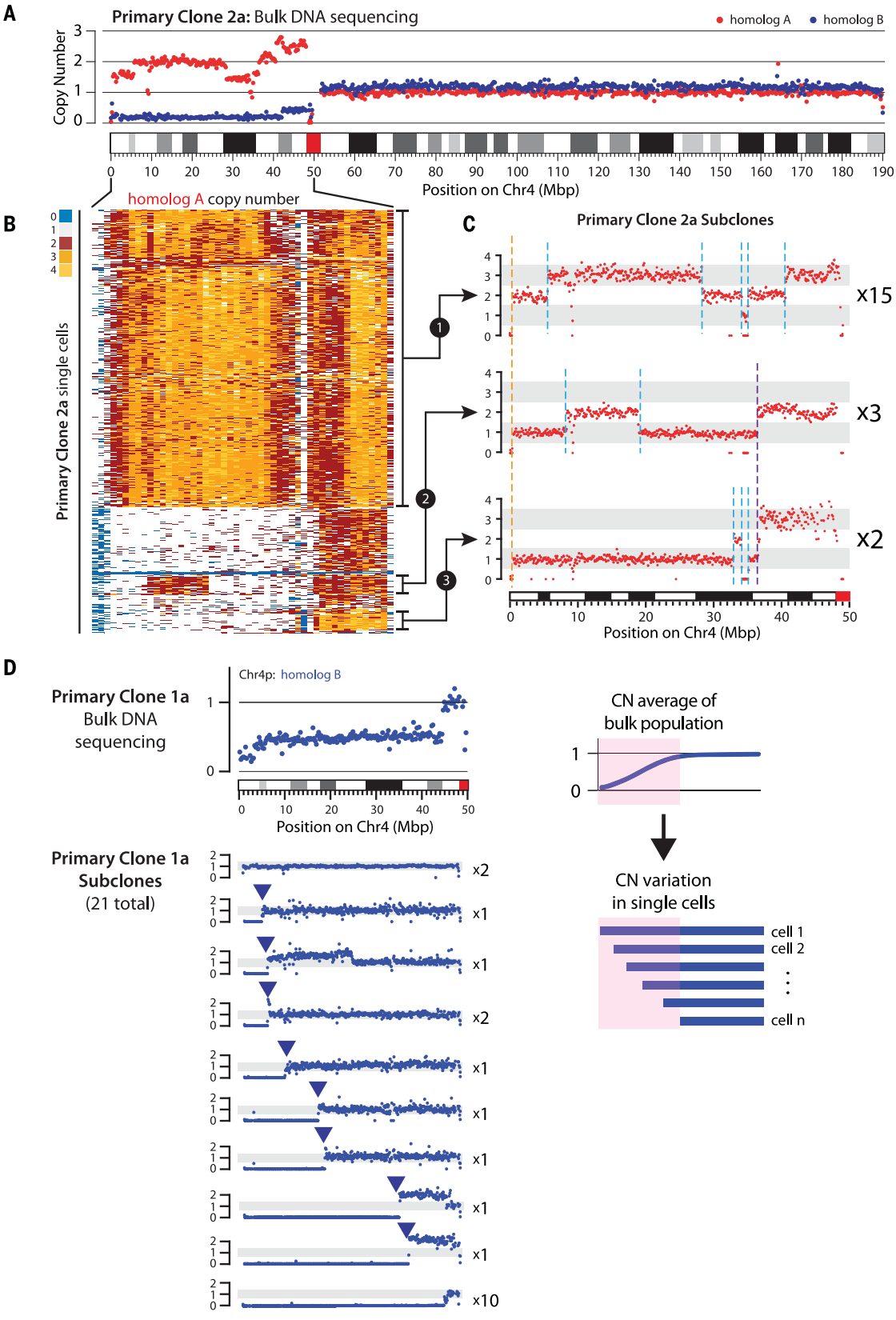

Fig. 7. Ongoing instability and subclonal heterogeneity after chromosome bridge formation. (**A**) Bulk sequencing indicates subclonal heterogeneity within a primary clone derived from a single cell after bridge breakage. The plot shows DNA copy number for the two Chr4 homologs (red and blue dots, 25-kb bins). Regions of noninteger copy number indicate the existence of subclones with different copy number states. (**B**) Copy-number heatmap for Chr4p (0 to 50 Mb) homolog A in 637 single cells. Each row represents one cell. Different subclonal populations can be identified that exhibit copy-number profiles consistent with those seen in single cell–derived subclones, shown in (C). (**C**) Copy-number profiles for Chr4p homolog A (red dots, 25-kb bins) in 20 subclones grown from single cells isolated from one primary clone. One copy-number transition (breakpoint) is shared by all subclones (dashed orange line), whereas other copy-number changes are shared only among a subset of subclones (dashed purple line) or are private to individual subclones (dashed cyan lines). The number of subclones represented in each copy-number profile is listed next to each plot. (**D**) Detection of ongoing chromosomal instability in a primary clone. (Top left) Copy number for Chr4p homolog B from bulk sequencing of the primary clone. (Bottom left) Ten different copy-number profiles identified from 21 single cell–derived subclones obtained from the primary clone. The number of subclones represented in each copy-number profile is listed next to each plot. (Right) Schematic shows how gradual sloping copy-number transitions in bulk populations are explained by subconal heterogeneity. CN, copy number.

generated during chromosome segregation in mitosis (*21*), cytokinetic furrow ingression, or abscission (*29*, *30*). However, it now appears that most bulky chromosome bridges are only broken after these events, during interphase (*33*). Interphase bridges were suggested to be cleaved enzymatically by means of a mechanism partially dependent on the cytoplasmic exonuclease TREX1 (*33*). However, our data disfavor a role for TREX1 and, instead, demonstrate that bridge breakage requires mechanical forces from the interphase actin cytoskeleton (Fig. 1). These forces appear to be exerted locally on DNA near the base of the bridge and are associated with transient actomyosin accumulation and large focal adhesions. Actomyosin forces appear to be transmitted in part across the NE to the bridge chromatin by the LINC complex (*58*, *59*).

A simple interpretation of our results is that actomyosin-dependent forces are capable of rupturing the phosphodiester bonds in bridge DNA. The force required to break DNA (*60*, *61*) is estimated to be almost an order of magnitude lower than traction forces generated from individual focal adhesions (*40*, *62*–*64*). Although noncovalent interactions connecting actin to chromatin are expected to be individually weak, large numbers of attachments acting in parallel could support the high mechanical load needed to break DNA. It is also possible that bridge breakage involves DNA processing enzyme(s) whose activity or access to DNA is enhanced by mechanical tension. Additionally, actomyosin-mediated disruption of NE integrity could enable access of cytoplasmic nucleases to bridge DNA. However, we did not detect an impact of NE rupture on bridge breakage, which generally disfavors a mechanism based on NE-restricted access of cytoplasmic nucleases to bridge DNA. We therefore propose that mechanical force is either sufficient for DNA breakage or facilitates the action of one or more nuclear-localized factors, such as a nuclease or topoisomerase.

Single-cell sequencing after chromosome bridge breakage identified either simple breaks or local DNA fragmentation, which is consistent with a breakage mechanism involving mechanical force. We also observed both simple breakage and fragmentation when we mechanically broke intact chromosome bridges with a glass capillary. In principle, mechanical bridge breakage could cause localized chromosome fragmentation if forces were applied to multiple sites on chromatin, such as might occur if chromatin were in a looped conformation.

Chromosomal rearrangements from abnormal nuclear architecture

When bridge breakage was accompanied by fragmentation, we often observed chromosome rearrangements consistent with fragment religation. Depending on the degree of fragmentation, this generated a range of outcomes (Fig. 3), from simpler patterns similar to the local jump footprint described in cancer genomes (*44*) to more complex events meeting conventional criteria for chromothripsis (supplementary materials, supplementary text) (*65*).

A subset of bridge-breakage events (4 of 20) showed a distinct pattern of extreme localized rearrangements, in which small (~1 to 10 kb) regions contained focal clusters of ~10 breakpoints each. These hotspots were extensively interconnected by rearrangements, despite being situated megabases apart in the reference genome or, occasionally, on different chromosomes. This generated a signature of multiple short (~200 bp) insertions present in tandem within rearrangement junctions (TST jumps) (Fig. 5). One possible model is that TST jumps are generated by aberrant DNA replication involving replication template switching (*12*). First, local breakpoint clusters are not expected from a random fragmentation process but could be generated by localized cycles of replication fork collapse, breakage, and error-prone replicative repair. Second, the size distribution of inserted segments (fig. S10B) seems inconsistent with random fragmentation and religation. Consistent with micronuclei and chromosome bridges having similar functional defects, we previously identified an example of multiple short tandem insertions in single-cell analysis of chromothripsis derived from a micronucleus (*17*).

The TST jump signature does not result from artifacts during single-cell whole-genome amplification because a similar pattern was observed in bulk sequencing analysis of clonal populations of cells after bridge breakage. Furthermore, we observed a similar signature by means of single-molecule long-read sequencing of a renal cell carcinoma genome. Features of the TST jump signature have been noted in a variety of other contexts (*44*, *66*, *67*), although never previously fully defined, including lung cancer and in populations of cells deficient in nonhomologous end-joining that emerged from telomere crisis (*68*), indicating that TST jumps may be common in cancer genomes. Although the cause of the TST jump signature is unknown, the restricted size distribution of the insertions might be generated by a low-processivity DNA polymerase or possibly by the use of Okazaki fragments as replication templates.

We observed similar DNA replication abnormalities occurring in chromosome bridges and intact micronuclei. This makes sense because both nuclear structures have a similar defect in NE assembly (*19*), which should generate a similarly defective nucleoplasm. In general, DNA replication errors are thought to be major sources of structural variation in cancer genomes. However, what triggers these severe replication abnormalities in the first place remains poorly understood. We propose that nuclear architecture defects, a hallmark feature of cancer termed nuclear atypia (*69*), are a major trigger for cancer-associated DNA replication errors.

A second wave of DNA damage from aberrant mitotic DNA replication

We uncovered an unexpected burst of DNA replication that occurs during mitosis, specifically on the stubs of broken chromosome bridges or on micronuclear chromosomes. In contrast with a previously reported form of mitotic replication that is beneficial for cells (*70*), the mitotic DNA replication described in our study is highly aberrant and produces heavy DNA damage and ssDNA formation.

The mechanism that triggers mitotic DNA replication on bridge stubs or micronuclear chromosomes is not known. However, because bridge and micronuclear DNA is incompletely replicated during interphase, these structures likely contain stalled DNA replication forks and licensed replication origins that have not fired. We previously found that incomplete DNA replication in micronuclei occurs because of defective nucleocytoplasmic transport, leading to a failure to accumulate key proteins required for DNA replication and repair (*4*, *14*, *19*). However, when cells enter mitosis, the NE is broken down, and under-replicated bridge or micronuclear DNA will suddenly gain access to the pool of replication factors that were sequestered in the primary nucleus throughout interphase. Access to replication factors, coupled with high mitotic CDK activity (*71*), likely then triggers mitotic replication of this incompletely replicated DNA. The DNA damage correlated with mitotic DNA replication may have a number of causes, including the well-described activation of structure-specific endonucleases in mitosis (*25*) and/or the recently discovered cleavage of stalled DNA replication forks that occurs because of removal of the MCM2-7 replicative helicase from mitotic chromosomes (*72*, *73*).

Chromosome bridges generate micronuclei

We found that chromosome bridge formation predisposes to micronucleation, which could then initiate additional rounds of chromothripsis downstream of bridge breakage (*14*, *17*, *74*). Because bridge breakage usually generates micronuclei with a centromere-containing chromosome fragment, it appears that bridge formation or breakage compromises centromere-kinetochore function. The mechanism for this centromere inactivation remains an interesting open question. Because stretching of chromosome bridges causes histone ejection (*33*, *75*), we speculate that actomyosin forces could also strip centromere-associated protein A (CENP-A)–containing nucleosomes when centromeric chromatin is trapped within the bridge. Thus,

in addition to promoting mutagenesis, actomyosin contractility may disrupt epigenetic marks on chromatin.

Rapid genome evolution from a single cell division error

The above-described cascade of events is predicted to generate ongoing cycles of complex genome evolution, a hypothesis that we tested with a CRISPR-based system to track the fate of a defined chromosome bridge over many generations. In these populations, we detected extensive genetic heterogeneity, with evidence that complex rearrangement continually recurs downstream of bridge breakage.

Together, our findings identify mechanisms that explain the remarkable potential of a single unrepaired DNA break to compromise the integrity of the genome. In human cells, a single DNA break has little capacity to activate the DNA damage checkpoint or cause cell cycle arrest (*76*, *77*). An unrepaired break can therefore lead to many additional breaks because of the generation of micronuclei or additional chromosome bridges after cell division. Because de novo telomere addition is inefficient (*78*), stable end-capping of chromosomes is primarily achieved through chromosome translocation or break-induced DNA replication (*79*). An additional constraint is that the rearranged chromosome must contain only one functional centromere. The end result is that downstream of chromosome bridge formation, the accumulating burden of DNA breakage can easily exceed the capacity to stabilize broken chromosome ends. Therefore, complex genome evolution with subclonal heterogeneity is virtually an inevitable consequence of chromosome bridge formation, itself a common outcome of cell division defects during tumorigenesis.

Methods summary

Cell culture, drug treatments, and imaging were performed essentially as described (supplementary materials, materials and methods) (*17*). Look-Seq experiments were performed as described (*17*), with the exception that a CellEctor system (Molecular Machines & Industries) was used in most cases for cell isolation. For long-term evolution experiments, we used the Look-Seq procedure with the following modifications. After bridge breakage, single cells were isolated into 96-well culture plates and then grown into large populations ($<10^6$ cells each). Cells were then taken from the populations for karyotyping, bulk sequencing, and single-cell copy-number analysis with the Chromium kit (10X Genomics). In some cases, single cells from populations were flow-sorted into 96-well culture plates for subcloning, followed by bulk sequencing. Single-cell genome amplification, sequencing library construction, and whole-genome sequencing were done as described (*17*), except that most sequencing was done on the NovaSeq platform.

REFERENCES AND NOTES

1. ICGC/TCGA Pan-Cancer Analysis of Whole Genomes Consortium, Pan-cancer analysis of whole genomes. *Nature* **578**, 82–93 (2020). doi: 10.1038/s41586-020-1969-6; pmid: 32025007
2. I. Cortés-Ciriano *et al*., Comprehensive analysis of chromothripsis in 2,658 human cancers using whole-genome sequencing. *Nat. Genet.* **52**, 331–341 (2020). doi: 10.1038/s41588-019-0576-7; pmid: 32025003
3. T. Fujiwara *et al*., Cytokinesis failure generating tetraploids promotes tumorigenesis in p53-null cells. *Nature* **437**, 1043–1047 (2005). doi: 10.1038/nature04217; pmid: 16222300
4. M. L. Leibowitz, C. Z. Zhang, D. Pellman, Chromothripsis: A New Mechanism for Rapid Karyotype Evolution. *Annu. Rev. Genet.* **49**, 183–211 (2015). doi: 10.1146/annurev-genet-120213-092228; pmid: 26442848
5. P. Ly, D. W. Cleveland, Rebuilding chromosomes after catastrophe: Emerging mechanisms of chromothripsis. *Trends Cell Biol.* **27**, 917–930 (2017). doi: 10.1016/j.tcb.2017.08.005; pmid: 28899600
6. P. J. Stephens *et al*., Massive genomic rearrangement acquired in a single catastrophic event during cancer development. *Cell* **144**, 27–40 (2011). doi: 10.1016/j.cell.2010.11.055; pmid: 21215367
7. S. Turajlic, A. Sottoriva, T. Graham, C. Swanton, Resolving genetic heterogeneity in cancer. *Nat. Rev. Genet.* **20**, 404–416 (2019). doi: 10.1038/s41576-019-0114-6; pmid: 30918367
8. R. Gao *et al*., Punctuated copy number evolution and clonal stasis in triple-negative breast cancer. *Nat. Genet.* **48**, 1119–1130 (2016). doi: 10.1038/ng.3641; pmid: 27526321
9. S. M. A. Lens, R. H. Medema, Cytokinesis defects and cancer. *Nat. Rev. Cancer* **19**, 32–45 (2019). doi: 10.1038/s41568-018-0084-6; pmid: 30523339
10. T. I. Zack *et al*., Pan-cancer patterns of somatic copy number alteration. *Nat. Genet.* **45**, 1134–1140 (2013). doi: 10.1038/ng.2760; pmid: 24071852
11. S. C. Baca *et al*., Punctuated evolution of prostate cancer genomes. *Cell* **153**, 666–677 (2013). doi: 10.1016/j.cell.2013.03.021; pmid: 23622249
12. P. Liu *et al*., Chromosome catastrophes involve replication mechanisms generating complex genomic rearrangements. *Cell* **146**, 889–903 (2011). doi: 10.1016/j.cell.2011.07.042; pmid: 21925314
13. F. Notta *et al*., A renewed model of pancreatic cancer evolution based on genomic rearrangement patterns. *Nature* **538**, 378–382 (2016). doi: 10.1038/nature19823; pmid: 27732578
14. K. Crasta *et al*., DNA breaks and chromosome pulverization from errors in mitosis. *Nature* **482**, 53–58 (2012). doi: 10.1038/nature10802; pmid: 22258507
15. P. Ly *et al*., Selective Y centromere inactivation triggers chromosome shattering in micronuclei and repair by non-homologous end joining. *Nat. Cell Biol.* **19**, 68–75 (2017). doi: 10.1038/ncb3450; pmid: 27918550
16. P. N. Rao, R. T. Johnson, Premature chromosome condensation. *Academic Press*, (1982).
17. C. Z. Zhang *et al*., Chromothripsis from DNA damage in micronuclei. *Nature* **522**, 179–184 (2015). doi: 10.1038/nature14493; pmid: 26017310
18. E. M. Hatch, A. H. Fischer, T. J. Deerinck, M. W. Hetzer, Catastrophic nuclear envelope collapse in cancer cell micronuclei. *Cell* **154**, 47–60 (2013). doi: 10.1016/j.cell.2013.06.007; pmid: 23827674
19. S. Liu *et al*., Nuclear envelope assembly defects link mitotic errors to chromothripsis. *Nature* **561**, 551–555 (2018). doi: 10.1038/s41586-018-0534-z; pmid: 30232450
20. B. McClintock, The behavior in successive nuclear divisions of a chromosome broken at meiosis. *Proc. Natl. Acad. Sci. U.S.A.* **25**, 405–416 (1939). doi: 10.1073/pnas.25.8.405; pmid: 16577924
21. B. McClintock, The stability of broken ends of chromosomes in *Zea mays*. *Genetics* **26**, 234–282 (1941). pmid: 17247004
22. B. van Steensel, A. Smogorzewska, T. de Lange, TRF2 protects human telomeres from end-to-end fusions. *Cell* **92**, 401–413 (1998). doi: 10.1016/S0092-8674(00)80932-0; pmid: 9476899
23. T. A. Hartl, S. J. Sweeney, P. J. Knepler, G. Bosco, Condensin II resolves chromosomal associations to enable anaphase I segregation in *Drosophila* male meiosis. *PLOS Genet.* **4**, e1000228 (2008). doi: 10.1371/journal.pgen.1000228; pmid: 18927632
24. C. F. Nielsen *et al*., PICH promotes sister chromatid disjunction and co-operates with topoisomerase II in mitosis. *Nat. Commun.* **6**, 8962 (2015). doi: 10.1038/ncomms9962; pmid: 26643143
25. S. C. West *et al*., Resolution of recombination intermediates: Mechanisms and regulation. *Cold Spring Harb. Symp. Quant. Biol.* **80**, 103–109 (2015). doi: 10.1101/sqb.2015.80.027649; pmid: 26370409
26. Y. Li *et al*., Constitutional and somatic rearrangement of chromosome 21 in acute lymphoblastic leukaemia. *Nature* **508**, 98–102 (2014). doi: 10.1038/nature13115; pmid: 24670643
27. D. W. Garsed *et al*., The architecture and evolution of cancer neochromosomes. *Cancer Cell* **26**, 653–667 (2014). doi: 10.1016/j.ccell.2014.09.010; pmid: 25517748
28. B. R. Mardin *et al*., A cell-based model system links chromothripsis with hyperploidy. *Mol. Syst. Biol.* **11**, 828 (2015). doi: 10.15252/msb.20156505; pmid: 26415501
29. J. G. Carlton, A. Caballe, M. Agromayor, M. Kloc, J. Martin-Serrano, ESCRT-III governs the Aurora B-mediated abscission checkpoint through CHMP4C. *Science* **336**, 220–225 (2012). doi: 10.1126/science.1217180; pmid: 22422861
30. A. Janssen, M. van der Burg, K. Szuhai, G. J. Kops, R. H. Medema, Chromosome segregation errors as a cause of DNA damage and structural chromosome aberrations. *Science* **333**, 1895–1898 (2011). doi: 10.1126/science.1210214; pmid: 21960636
31. M. Mendoza, Y. Barral, Co-ordination of cytokinesis with chromosome segregation. *Biochem. Soc. Trans.* **36**, 387–390 (2008). doi: 10.1042/BST0360387; pmid: 18481965
32. Y. Liu, C. F. Nielsen, Q. Yao, I. D. Hickson, The origins and processing of ultra fine anaphase DNA bridges. *Curr. Opin. Genet. Dev.* **26**, 1–5 (2014). doi: 10.1016/j.gde.2014.03.003; pmid: 24795279
33. J. Maciejowski, Y. Li, N. Bosco, P. J. Campbell, T. de Lange, Chromothripsis and kataegis induced by telomere crisis. *Cell* **163**, 1641–1654 (2015). doi: 10.1016/j.cell.2015.11.054; pmid: 26687355
34. P. Steigemann *et al*., Aurora B-mediated abscission checkpoint protects against tetraploidization. *Cell* **136**, 473–484 (2009). doi: 10.1016/j.cell.2008.12.020; pmid: 19203582
35. M. S. Lee, R. Craigie, A previously unidentified host protein protects retroviral DNA from autointegration. *Proc. Natl. Acad. Sci. U.S.A.* **95**, 1528–1533 (1998). doi: 10.1073/pnas.95.4.1528; pmid: 9465049
36. M. Théry, Micropatterning as a tool to decipher cell morphogenesis and functions. *J. Cell Sci.* **123**, 4201–4213 (2010). doi: 10.1242/jcs.075150; pmid: 21123618
37. A. Diz-Muñoz, D. A. Fletcher, O. D. Weiner, Use the force: Membrane tension as an organizer of cell shape and motility. *Trends Cell Biol.* **23**, 47–53 (2013). doi: 10.1016/j.tcb.2012.09.006; pmid: 23122885
38. D. A. Lauffenburger, A. F. Horwitz, Cell migration: A physically integrated molecular process. *Cell* **84**, 359–369 (1996). doi: 10.1016/S0092-8674(00)81280-5; pmid: 8608589
39. S. Miyamoto, B. Z. Katz, R. M. Lafrenie, K. M. Yamada, Fibronectin and integrins in cell adhesion, signaling, and morphogenesis. *Ann. N. Y. Acad. Sci.* **857**, 119–129 (1998). doi: 10.1111/j.1749-6632.1998.tb10112.x; pmid: 9917837
40. A. Saez, A. Buguin, P. Silberzan, B. Ladoux, Is the mechanical activity of epithelial cells controlled by deformations or forces? *Biophys. J.* **89**, L52–L54 (2005). doi: 10.1529/biophysj.105.071217; pmid: 16214867
41. D. A. Starr, H. N. Fridolfsson, Interactions between nuclei and the cytoskeleton are mediated by SUN-KASH nuclear-envelope bridges. *Annu. Rev. Cell Dev. Biol.* **26**, 421–444 (2010). doi: 10.1146/annurev-cellbio-100109-104037; pmid: 20507227
42. B. McClintock, Chromosome organization and genic expression. *Cold Spring Harb. Symp. Quant. Biol.* **16**, 13–47 (1951). doi: 10.1101/SQB.1951.016.01.004; pmid: 14942727
43. A. Smogorzewska, J. Karlseder, H. Holtgreve-Grez, A. Jauch, T. de Lange, DNA ligase IV-dependent NHEJ of deprotected mammalian telomeres in G_1 and G_2. *Curr. Biol.* **12**, 1635–1644 (2002). doi: 10.1016/S0960-9822(02)01179-X; pmid: 12361565
44. Y. Li *et al*., Patterns of somatic structural variation in human cancer genomes. *Nature* **578**, 112–121 (2020). doi: 10.1038/s41586-019-1913-9; pmid: 32025012
45. S. Nik-Zainal *et al*., Mutational processes molding the genomes of 21 breast cancers. *Cell* **149**, 979–993 (2012). doi: 10.1016/j.cell.2012.04.024; pmid: 22608084
46. S. A. Roberts *et al*., Clustered mutations in yeast and in human cancers can arise from damaged long single-strand DNA

regions. *Mol. Cell* **46**, 424–435 (2012). doi: 10.1016/j.molcel.2012.03.030; pmid: 22607975
47. F. Zhang *et al*., The DNA replication FoSTeS/MMBIR mechanism can generate genomic, genic and exonic complex rearrangements in humans. *Nat. Genet.* **41**, 849–853 (2009). doi: 10.1038/ng.399; pmid: 19543269
48. R. P. Anand *et al*., Chromosome rearrangements via template switching between diverged repeated sequences. *Genes Dev.* **28**, 2394–2406 (2014). doi: 10.1101/gad.250258.114; pmid: 25367035
49. T. J. Mitchell *et al*., Timing the landmark events in the evolution of clear cell renal cell cancer: TRACERx renal. *Cell* **173**, 611–623.e17 (2018). doi: 10.1016/j.cell.2018.02.020; pmid: 29656891
50. L. Costantino *et al*., Break-induced replication repair of damaged forks induces genomic duplications in human cells. *Science* **343**, 88–91 (2014). doi: 10.1126/science.1243211; pmid: 24310611
51. J. Kramara, B. Osia, A. Malkova, Break-induced replication: The where, the why, and the how. *Trends Genet.* **34**, 518–531 (2018). doi: 10.1016/j.tig.2018.04.002; pmid: 29735283
52. D. R. Hoffelder *et al*., Resolution of anaphase bridges in cancer cells. *Chromosoma* **112**, 389–397 (2004). doi: 10.1007/s00412-004-0284-6; pmid: 15156327
53. D. Gisselsson *et al*., Chromosomal breakage-fusion-bridge events cause genetic intratumor heterogeneity. *Proc. Natl. Acad. Sci. U.S.A.* **97**, 5357–5362 (2000). doi: 10.1073/pnas.090013497; pmid: 10805796
54. K. M. Stimpson *et al*., Telomere disruption results in non-random formation of de novo dicentric chromosomes involving acrocentric human chromosomes. *PLOS Genet.* **6**, e1001061 (2010). doi: 10.1371/journal.pgen.1001061; pmid: 20711355
55. D. O. Warmerdam, R. M. F. Wolthuis, Keeping ribosomal DNA intact: A repeating challenge. *Chromosome Res.* **27**, 57–72 (2019). doi: 10.1007/s10577-018-9594-z; pmid: 30556094
56. B. McClintock, Spontaneous alterations in chromosome size and form in *Zea mays*. *Cold Spring Harb. Symp. Quant. Biol.* **9**, 72–81 (1941). doi: 10.1101/SQB.1941.009.01.010
57. L. R. Gehlen *et al*., Nuclear geometry and rapid mitosis ensure asymmetric episome segregation in yeast. *Curr. Biol.* **21**, 25–33 (2011). doi: 10.1016/j.cub.2010.12.016; pmid: 21194950
58. M. Crisp *et al*., Coupling of the nucleus and cytoplasm: Role of the LINC complex. *J. Cell Biol.* **172**, 41–53 (2006). doi: 10.1083/jcb.200509124; pmid: 16380439
59. T. Takaki *et al*., Actomyosin drives cancer cell nuclear dysmorphia and threatens genome stability. *Nat. Commun.* **8**, 16013 (2017). doi: 10.1038/ncomms16013; pmid: 28737169
60. D. Bensimon, A. J. Simon, V. Croquette, A. Bensimon, Stretching DNA with a receding meniscus: Experiments and models. *Phys. Rev. Lett.* **74**, 4754–4757 (1995). doi: 10.1103/PhysRevLett.74.4754; pmid: 10058590
61. M. Grandbois, M. Beyer, M. Rief, H. Clausen-Schaumann, H. E. Gaub, How strong is a covalent bond? *Science* **283**, 1727–1730 (1999). doi: 10.1126/science.283.5408.1727; pmid: 10073936
62. N. Q. Balaban *et al*., Force and focal adhesion assembly: A close relationship studied using elastic micropatterned substrates. *Nat. Cell Biol.* **3**, 466–472 (2001). doi: 10.1038/35074532; pmid: 11331874
63. O. du Roure *et al*., Force mapping in epithelial cell migration. *Proc. Natl. Acad. Sci. U.S.A.* **102**, 2390–2395 (2005). doi: 10.1073/pnas.0408482102; pmid: 15695588
64. J. L. Tan *et al*., Cells lying on a bed of microneedles: An approach to isolate mechanical force. *Proc. Natl. Acad. Sci. U.S.A.* **100**, 1484–1489 (2003). doi: 10.1073/pnas.0235407100; pmid: 12552122
65. J. O. Korbel, P. J. Campbell, Criteria for inference of chromothripsis in cancer genomes. *Cell* **152**, 1226–1236 (2013). doi: 10.1016/j.cell.2013.02.023; pmid: 23498933
66. J. J. Lee *et al*., Tracing oncogene rearrangements in the mutational history of lung adenocarcinoma. *Cell* **177**, 1842–1857.e21 (2019). doi: 10.1016/j.cell.2019.05.013; pmid: 31155235
67. J. A. Wala *et al*., SvABA: Genome-wide detection of structural variants and indels by local assembly. *Genome Res.* **28**, 581–591 (2018). doi: 10.1101/gr.221028.117; pmid: 29535149
68. K. Cleal, R. E. Jones, J. W. Grimstead, E. A. Hendrickson, D. M. Baird, Chromothripsis during telomere crisis is independent of NHEJ, and consistent with a replicative origin. *Genome Res.* **29**, 737–749 (2019). doi: 10.1101/gr.240705.118; pmid: 30872351
69. D. Zink, A. H. Fischer, J. A. Nickerson, Nuclear structure in cancer cells. *Nat. Rev. Cancer* **4**, 677–687 (2004). doi: 10.1038/nrc1430; pmid: 15343274
70. S. Minocherhomji *et al*., Replication stress activates DNA repair synthesis in mitosis. *Nature* **528**, 286–290 (2015). doi: 10.1038/nature16139; pmid: 26633632
71. S. P. Bell, A. Dutta, DNA replication in eukaryotic cells. *Annu. Rev. Biochem.* **71**, 333–374 (2002). doi: 10.1146/annurev.biochem.71.110601.135425; pmid: 12045100
72. L. Deng *et al*., Mitotic CDK promotes replisome disassembly, fork breakage, and complex DNA rearrangements. *Mol. Cell* **73**, 915–929.e6 (2019). doi: 10.1016/j.molcel.2018.12.021; pmid: 30849395
73. S. Priego Moreno, R. M. Jones, D. Poovathumkadavil, S. Scaramuzza, A. Gambus, Mitotic replisome disassembly depends on TRAIP ubiquitin ligase activity. *Life Sci. Alliance* **2**, e201900390 (2019). doi: 10.26508/lsa.201900390; pmid: 30979826
74. P. Ly *et al*., Chromosome segregation errors generate a diverse spectrum of simple and complex genomic rearrangements. *Nat. Genet.* **51**, 705–715 (2019). doi: 10.1038/s41588-019-0360-8; pmid: 30833795
75. M. L. Bennink *et al*., Unfolding individual nucleosomes by stretching single chromatin fibers with optical tweezers. *Nat. Struct. Biol.* **8**, 606–610 (2001). doi: 10.1038/89646; pmid: 11427891
76. D. Deckbar *et al*., Chromosome breakage after G_2 checkpoint release. *J. Cell Biol.* **176**, 749–755 (2007). doi: 10.1083/jcb.200612047; pmid: 17353355
77. J. van den Berg *et al*., A limited number of double-strand DNA breaks is sufficient to delay cell cycle progression. *Nucleic Acids Res.* **46**, 10132–10144 (2018). doi: 10.1093/nar/gky786; pmid: 30184135
78. C. Ribeyre, D. Shore, Regulation of telomere addition at DNA double-strand breaks. *Chromosoma* **122**, 159–173 (2013). doi: 10.1007/s00412-013-0404-2; pmid: 23504035
79. R. L. Dilley *et al*., Break-induced telomere synthesis underlies alternative telomere maintenance. *Nature* **539**, 54–58 (2016). doi: 10.1038/nature20099; pmid: 27760120
80. M. Krzywinski *et al*., Circos: An information aesthetic for comparative genomics. *Genome Res.* **19**, 1639–1645 (2009). doi: 10.1101/gr.092759.109; pmid: 19541911
81. D. Pellman, N. Umbreit, L. Blaine, R. Tourdot, H. Almubarak, C.-Z. Zhang, L. Sun, L. Lynch, A. Cheng, A. Spektor, T. Mitchell, K. Judge, Somatic copy number and structural variation in RPE-1 cells with induced chromosomal instability. Dryad (2020); doi: 10.5061/dryad.rn8pk0p61

ACKNOWLEDGMENTS

We thank M. Bao, P. Campbell, M. Kwon, J. Lee, S. Liu, M. Meyerson, J. Walter, and K. Xie for comments on the manuscript; I. Cheeseman, J. Maciejowski, and T. de Lange for reagents; and P. Campbell, J. Maciejowski, and T. de Lange for sharing unpublished results. **Funding:** N.T.U. was a Howard Hughes Medical Institute (HHMI) fellow of the Damon Runyon Cancer Institute and is supported by the Claudia Adams Barr Program for Innovative Cancer Research. T.J.M. is supported by Cancer Research UK and the Royal College of Surgeons (C63474/A27176). C.-Z.Z. is supported by a National Cancer Institute (NCI) career transition award (K22CA216319). R.T. and L.S. are supported by a NCI Cancer Moonshot award (1R33CA225344.). R.T. and H.F.A. are supported by the Harvard University Milton Fund. A.S. is supported by a NCI Mentored Clinical Scientist Research Career Development Award (K08CA208008) and a Burroughs-Wellcome Career Award for Medical Scientists (CAMS). D.P. is a HHMI investigator and is supported by NIH grant GM083299, a Research Investigator Award from the Lustgarten Foundation, and an award from the G. Harold and Leila Y. Mathers Charitable Foundation. **Author contributions:** D.P., N.T.U., and C.-Z.Z. conceived the project. D.P. and N.T.U. designed the biological experiments, which were performed by A.M.C., L.D.L., and N.T.U.; D.P., N.T.U., and C.-Z.Z. designed the sequencing experiments, which were performed by L.S. and N.T.U.; C.-Z.Z. designed and performed the analysis of single-cell and bulk sequencing data of RPE-1 samples, with help from L.J.B. Low-pass single-cell CNV analysis was performed by R.T. and H.F.A.; T.J.M. and K.J. contributed the data and analysis in Fig. 5C. A.S. contributed the data in figs. S15C and S16D and to early experiments on the project. D.P. and N.T.U. wrote the manuscript with edits from other authors. **Competing interests:** C.-Z.Z is a scientific adviser for Pillar BioSciences. All other authors declare no competing interests. **Data and materials availability:** Allelic copy-number analysis and structural variant calls for all chromosomes from single-cell sequencing samples are available at Dryad (*81*). DNA sequencing data have been deposited to the Sequencing Read Archive (SRA) under BioProject PRJNA602546. Correspondence regarding biological experiments and requests for materials should be addressed to N.T.U. and D.P.; correspondence regarding sequencing analysis and requests for sequencing data should be addressed to C.-Z.Z.

SUPPLEMENTARY MATERIALS

science.sciencemag.org/content/368/6488/eaba0712/suppl/DC1
Materials and Methods
Supplementary Text
Figs. S1 to S23
Tables S1 to S3
References (*82*–*102*)
Movies S1 to S8

View/request a protocol for this paper from *Bio-protocol*.

1 November 2019; accepted 4 March 2020
10.1126/science.aba0712

Science

Mechanisms generating cancer genome complexity from a single cell division error

Neil T. Umbreit, Cheng-Zhong Zhang, Luke D. Lynch, Logan J. Blaine, Anna M. Cheng, Richard Tourdot, Lili Sun, Hannah F. Almubarak, Kim Judge, Thomas J. Mitchell, Alexander Spektor and David Pellman

Science **368** (6488), eaba0712.
DOI: 10.1126/science.aba0712

Genomic havoc from one fateful mistake

Many human tumors display scrambled genomes that arise from two distinct mutational processes. The first, the chromosome breakage-fusion-bridge (BFB) cycle, produces gene amplification and genomic instability. The second, chromothripsis, generates massive, clustered genomic rearrangements in one or a few chromosomes. Umbreit *et al.* hypothesized that these two processes are mechanistically related and tested this idea by recreating essential steps of the BFB cycle in cultured cells (see the Perspective by Paiano and Nussenzweig). They found that chromothripsis arises from a cascade of events that begins with aberrant chromosome bridge formation during mitosis, followed by chromosome fragmentation, DNA damage, chromosome missegregation, and the formation of micronuclei. They propose a model that explains how a single cell division error (chromosome bridge formation) can generate many hallmark features of cancer genomes.

Science, this issue p. 240; see also p. eaba0712